

Identification of Chemical Constituents in *Blumea balsamifera* Using UPLC–Q–Orbitrap HRMS and Evaluation of Their Antioxidant Activities

Liping Dai^{1,2}, Shengnan Cai^{1,2}, Dake Chu², Rui Pang², Jianhao Deng², Xilong Zheng^{1,*}

and Wei Dai^{2,*}

Figure S1. MS² fragmentation spectra (CID) of α,α -trehalose

Figure S2. MS² fragmentation spectra (CID) of D-(–)-fructose

Figure S3. MS² fragmentation spectra (CID) of gentisic acid 5-O- β -glucoside

Figure S4. MS² fragmentation spectra (CID) of caffeic acid

Figure S5. MS² fragmentation spectra (CID) of tuberonic acid glucoside

Figure S6. MS² fragmentation spectra (CID) of hemiphloin

Figure S7. MS² fragmentation spectra (CID) of taxifolin

Figure S8. MS² fragmentation spectra (CID) of rutin

Figure S9. MS² fragmentation spectra (CID) of quercetin-3 β -D-glucoside

Figure S10. MS² fragmentation spectra (CID) of quercetin

Figure S11. MS² fragmentation spectra (CID) of quercetin-3-Arabinoside

Figure S12. MS² fragmentation spectra (CID) of cynaroside

Figure S13. MS² fragmentation spectra (CID) of 1,3-Dicaffeoylquinic acid

Figure S14. MS² fragmentation spectra (CID) of chlorogenic acid

Figure S15. MS² fragmentation spectra (CID) of isorhamnetin-3-O-glucoside

Figure S16. MS² fragmentation spectra (CID) of 4-oxo-5-phenylpentanoic acid

Figure S17. MS² fragmentation spectra (CID) of eriodictyol

Figure S18. MS² fragmentation spectra (CID) of padmatin

Figure S19. MS² fragmentation spectra (CID) of isorhamnetin

Figure S20. MS² fragmentation spectra (CID) of naringenin

Figure S21. MS² fragmentation spectra (CID) of 7-O-Methylaromadendrin

Figure S22. MS² fragmentation spectra (CID) of aurantio-obtusin

Figure S23. MS² fragmentation spectra (CID) of fraxetin

Figure S24. MS² fragmentation spectra (CID) of hematoxylin

Figure S25. MS² fragmentation spectra (CID) of sakuranetin

Figure S26. MS² fragmentation spectra (CID) of aurantiamide acetate

Figure S27. MS² fragmentation spectra (CID) of cryptotanshinone

Figure S28. MS² fragmentation spectra (CID) of nootkatone

Figure S29. MS² fragmentation spectra (CID) of N-Phenyl-1-naphthylamine

Figure S30. MS² fragmentation spectra (CID) of tanshinone IIA

Figure S31. MS² fragmentation spectra (CID) of citroflex A-4

Figure S32. TICs of *Blumea balsamifera* (L.) DC. in negative ion mode

Figure S33. TICs of *Blumea balsamifera* (L.) DC. in positive ion mode

ANX-100%JC-Nd #952 RT: 0.86 AV: 1 NL: 2.55E5
F: FTMS - p ESId Full ms2 341.1084@hcd40.00 [50.0000-368.6956]

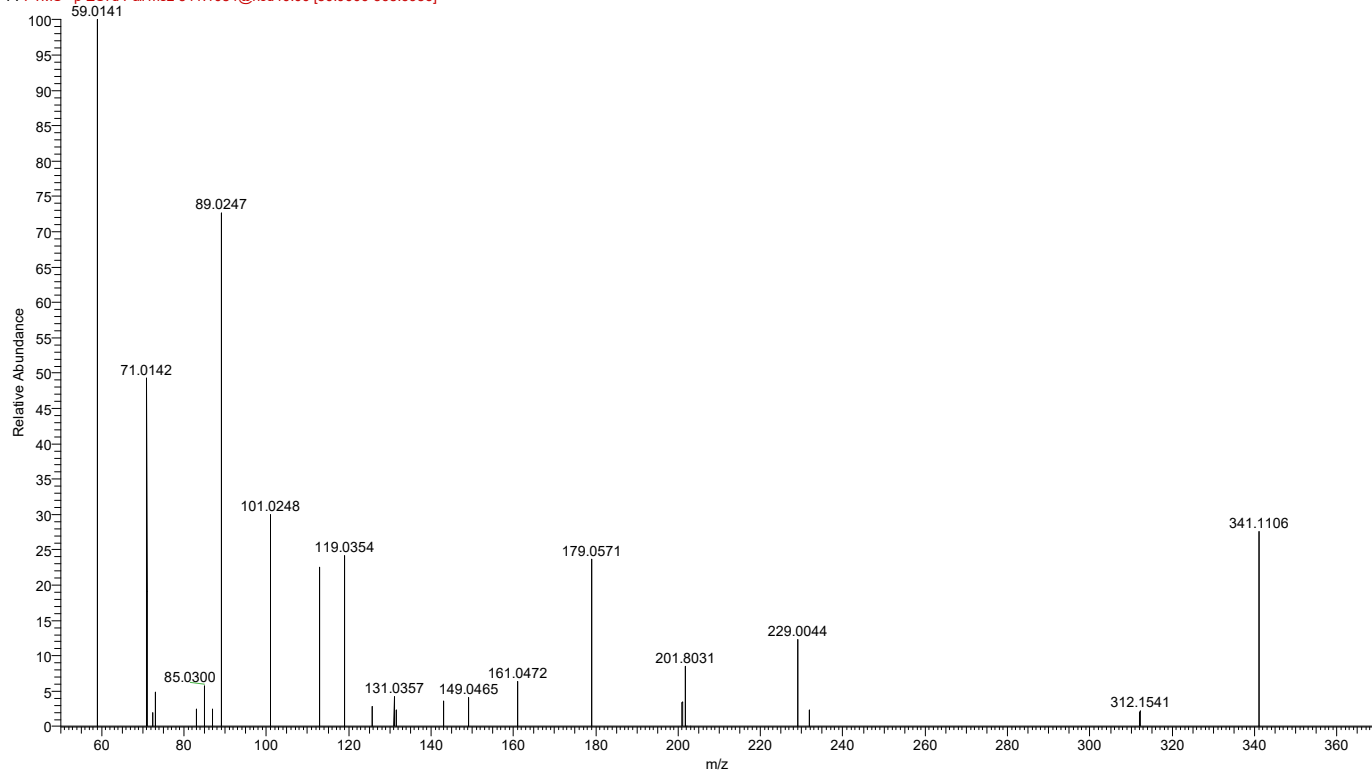


Figure S1. MS² fragmentation spectra (CID) of α,α -trehalose

ANX-100%JC-Nd #941 RT: 0.85 AV: 1 NL: 5.14E5
F: FTMS - p ESId Full ms2 179.0558@hcd40.00 [40.6804-203.4019]

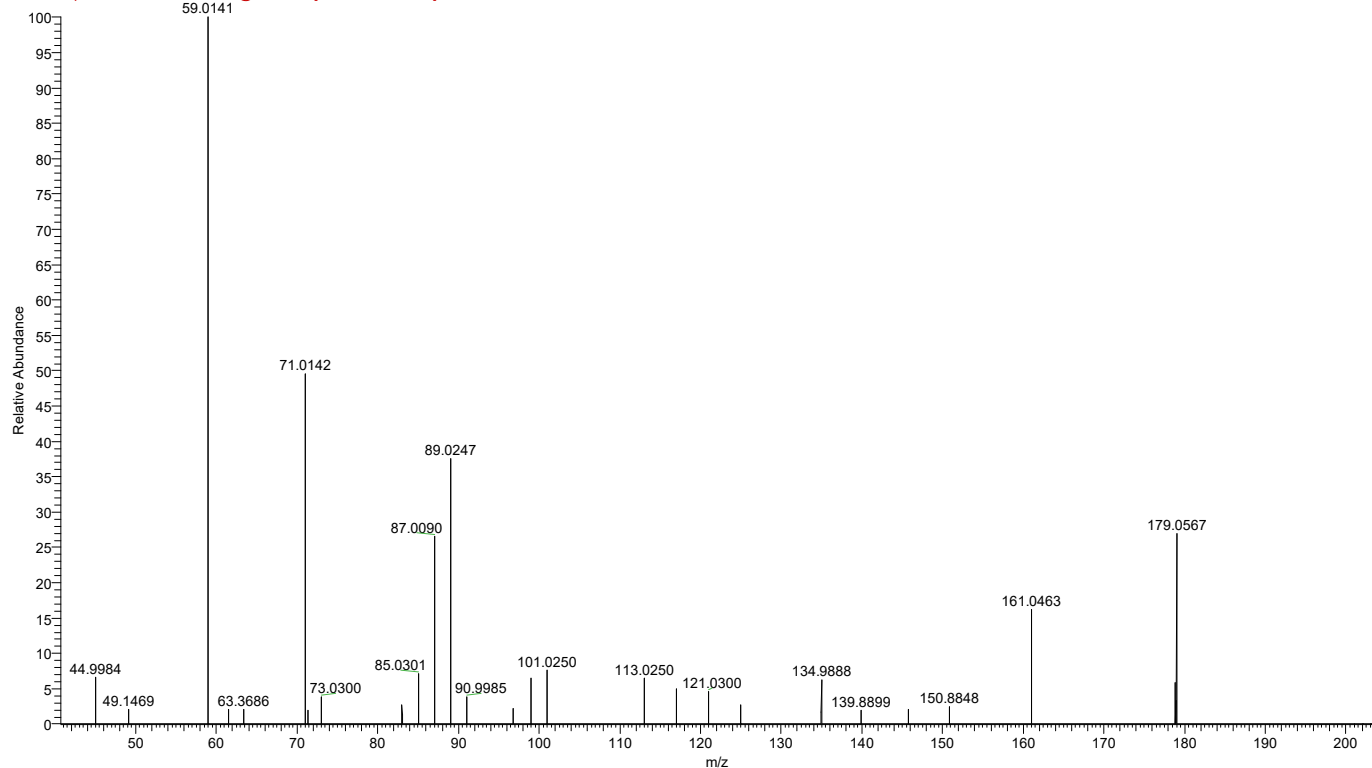


Figure S2. MS² fragmentation spectra (CID) of D-(-)-fructose

ANX-100%JC-Nd #2422 RT: 2.15 AV: 1 NL: 1.59E5
F: FTMS - p ESId Full ms2 315.0504@hcd40.00 [50.0000-342.1164]

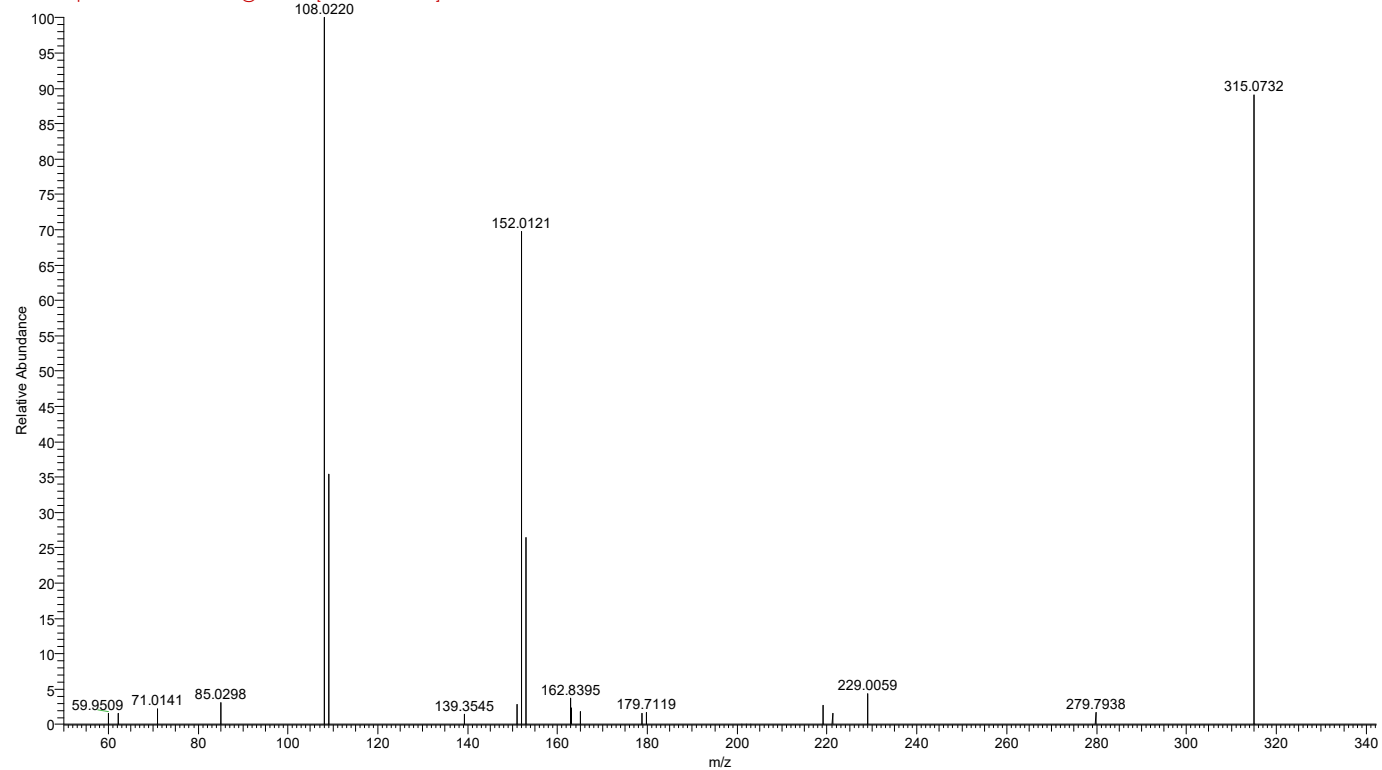


Figure S3. MS² fragmentation spectra (CID) of gentisic acid 5-O- β -glucoside

ANX-100%JC-Nd #6705 RT: 5.93 AV: 1 NL: 1.05E6
F: FTMS - p ESId Full ms2 179.0558@hcd40.00 [40.6804-203.4019]

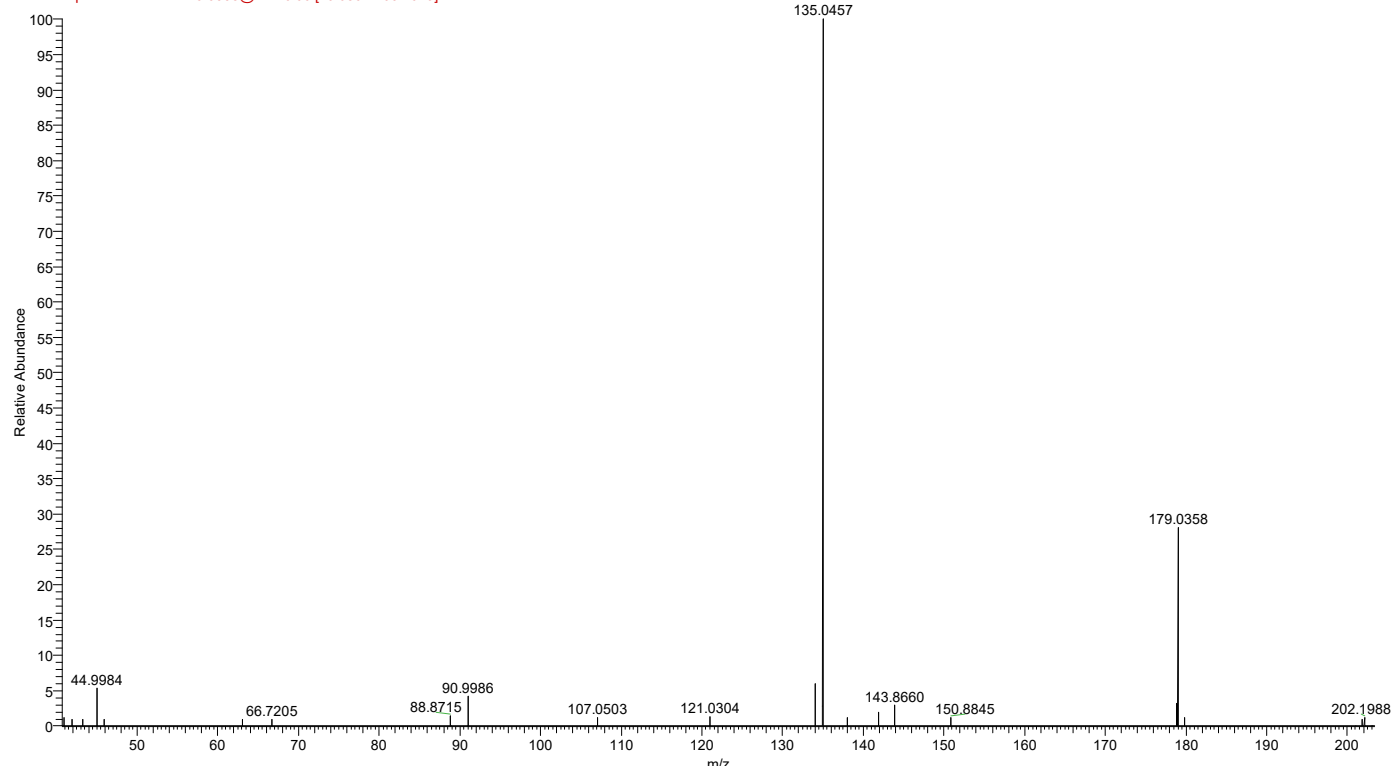


Figure S4. MS² fragmentation spectra (CID) of caffeoic acid

ANX-100%JC-Nd #8187 RT: 7.23 AV: 1 NL: 2.21E5
F: FTMS - p ESId Full ms2 387.1140@hcd40.00 [50.0000-415.6212]

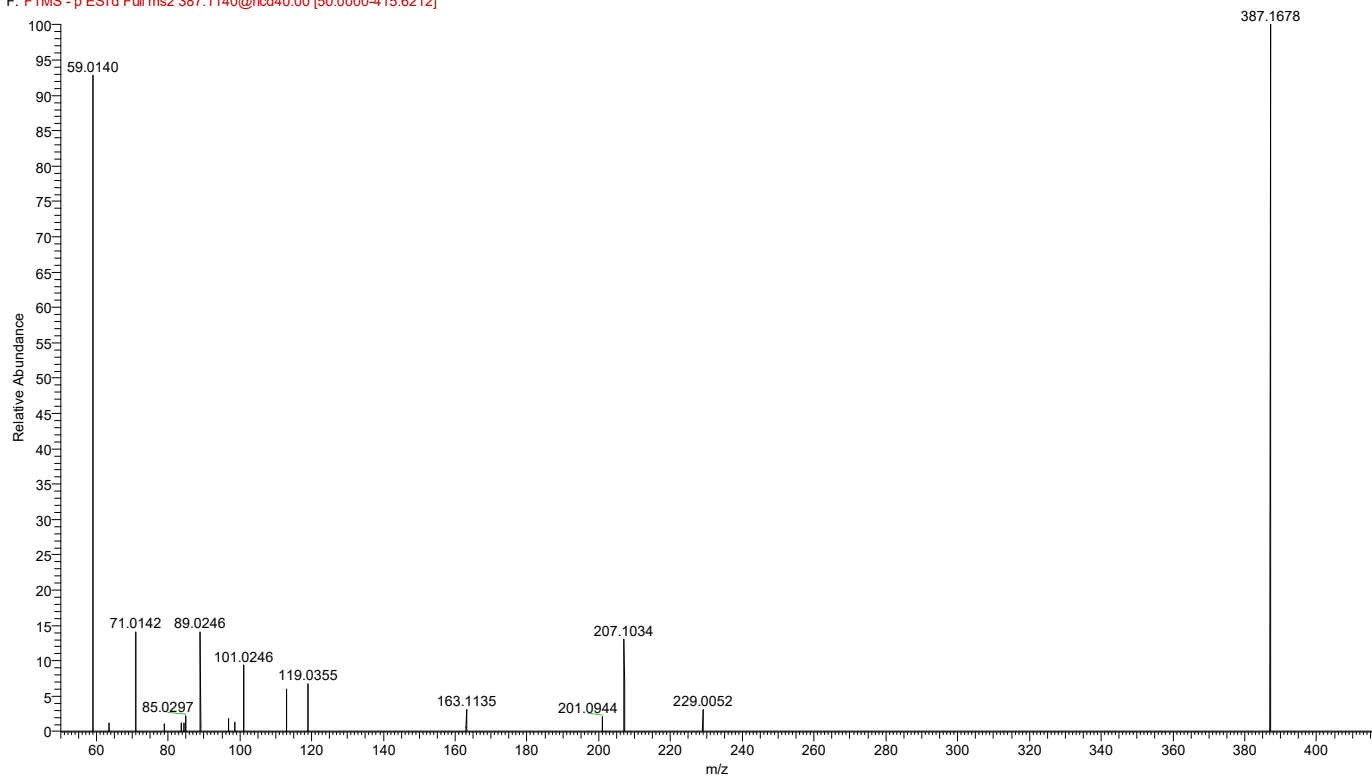


Figure S5. MS² fragmentation spectra (CID) of tuberonic acid glucoside

ANX-100%JC-Nd #11533 RT: 10.18 AV: 1 NL: 3.45E6
F: FTMS - p ESId Full ms2 433.1142@hcd40.00 [50.0000-462.5415]

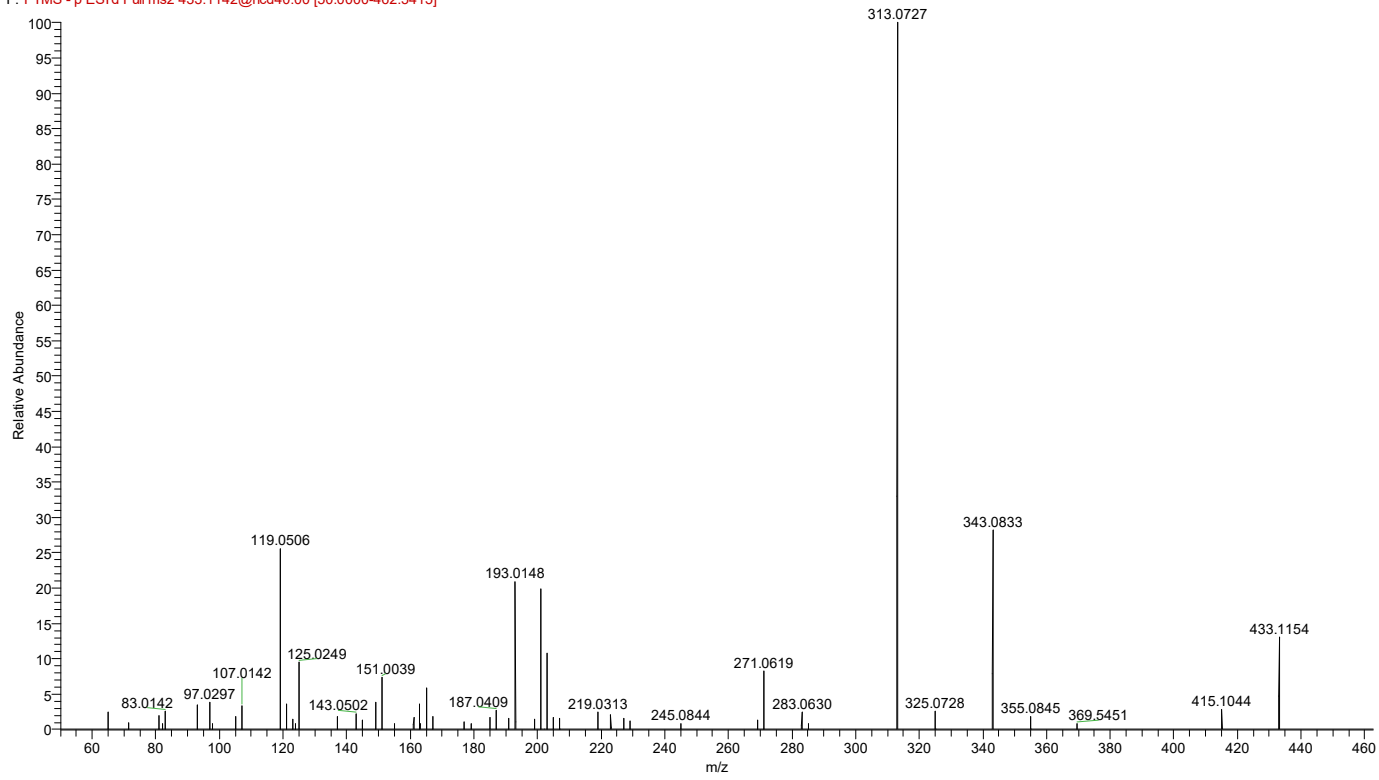


Figure S6. MS² fragmentation spectra (CID) of hemipholin

ANX-100%JC-Nd #111762 RT: 10.38 AV: 1 NL: 1.66E5
F: FTMS - p ESId Full ms2 303.1348@hcd40.00 [50.0000-329.9625]

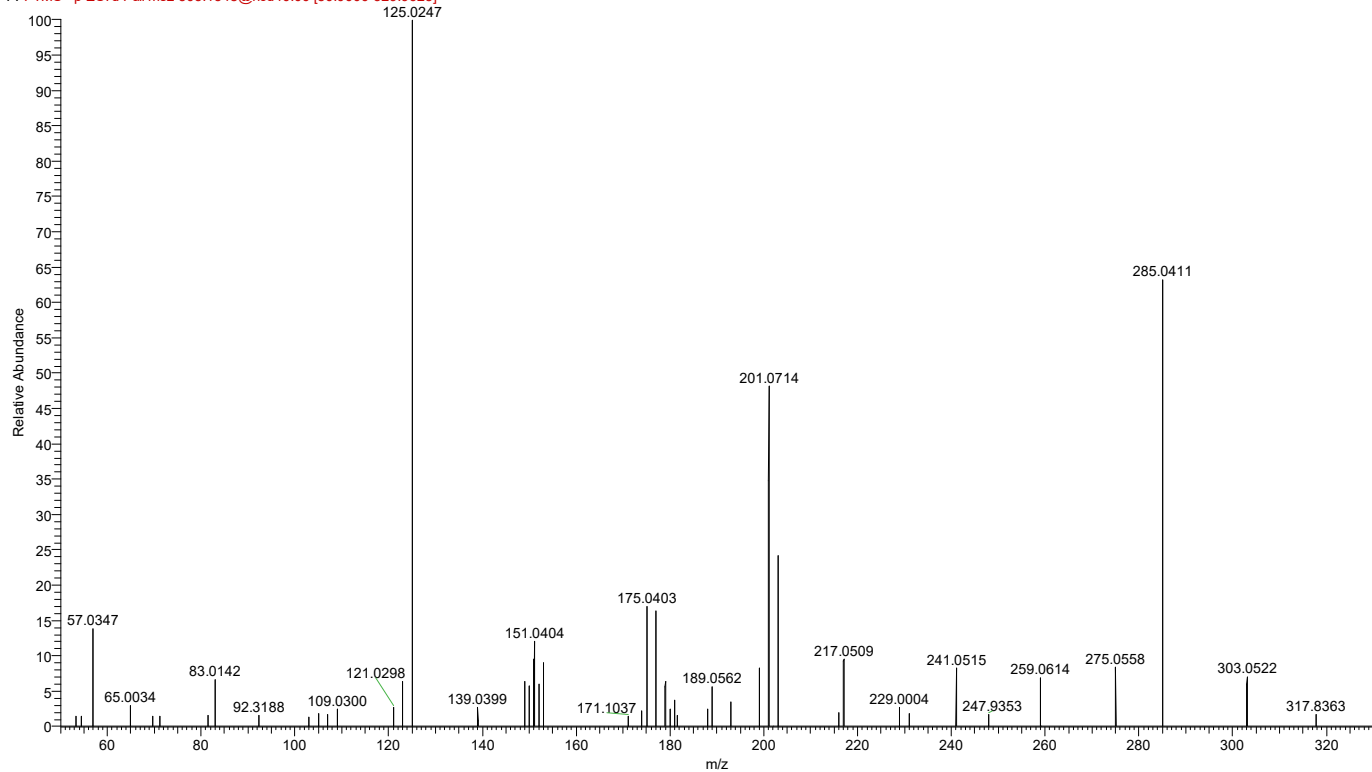


Figure S7. MS² fragmentation spectra (CID) of taxifolin

ANX-100%JC-Nd #111827 RT: 10.44 AV: 1 NL: 1.12E6
F: FTMS - p ESId Full ms2 609.1390@hcd40.00 [64.2087-642.0867]

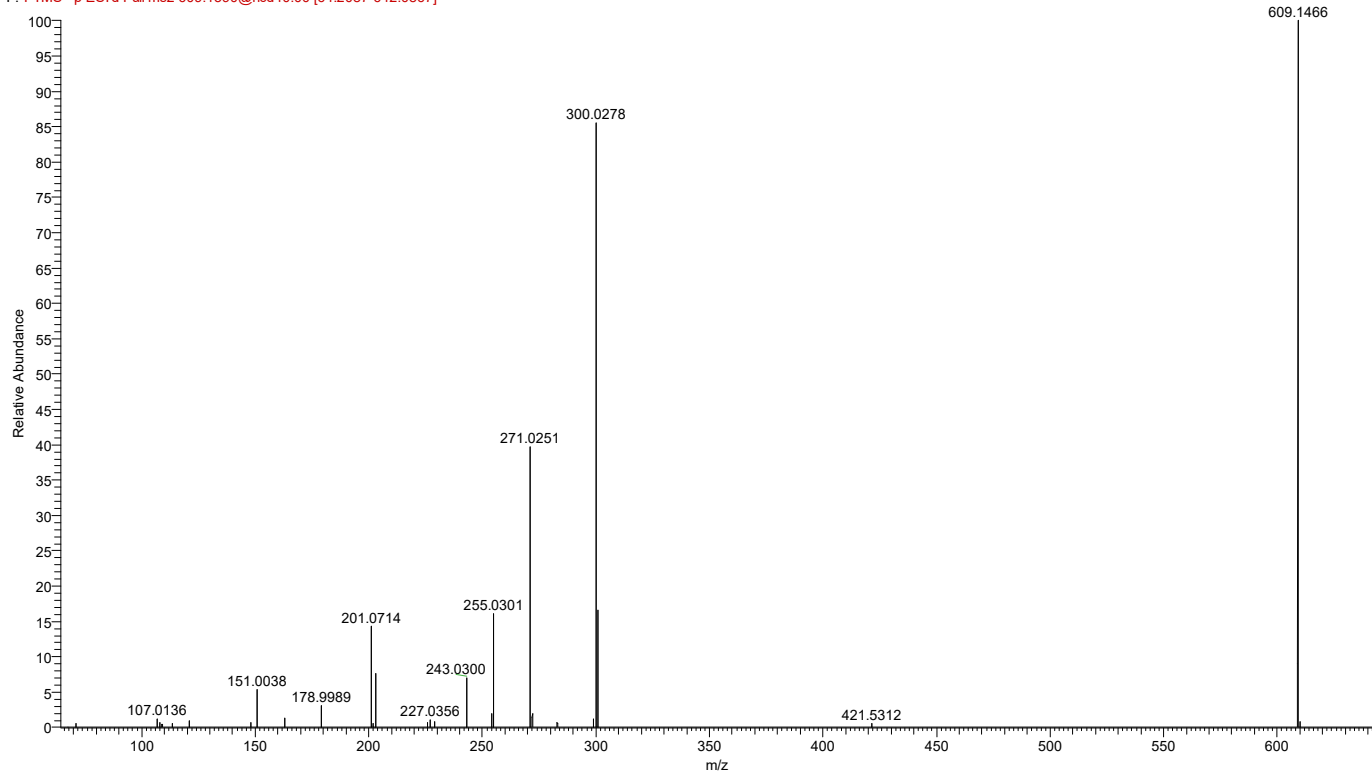


Figure S8. MS² fragmentation spectra (CID) of rutin

ANX-100%JC-Nd #12480 RT: 11.02 AV: 1 NL: 1.73E6
F: FTMS - p ESI:d Full ms2 463.0877@hcd40.00 [50.0000-493.1144]

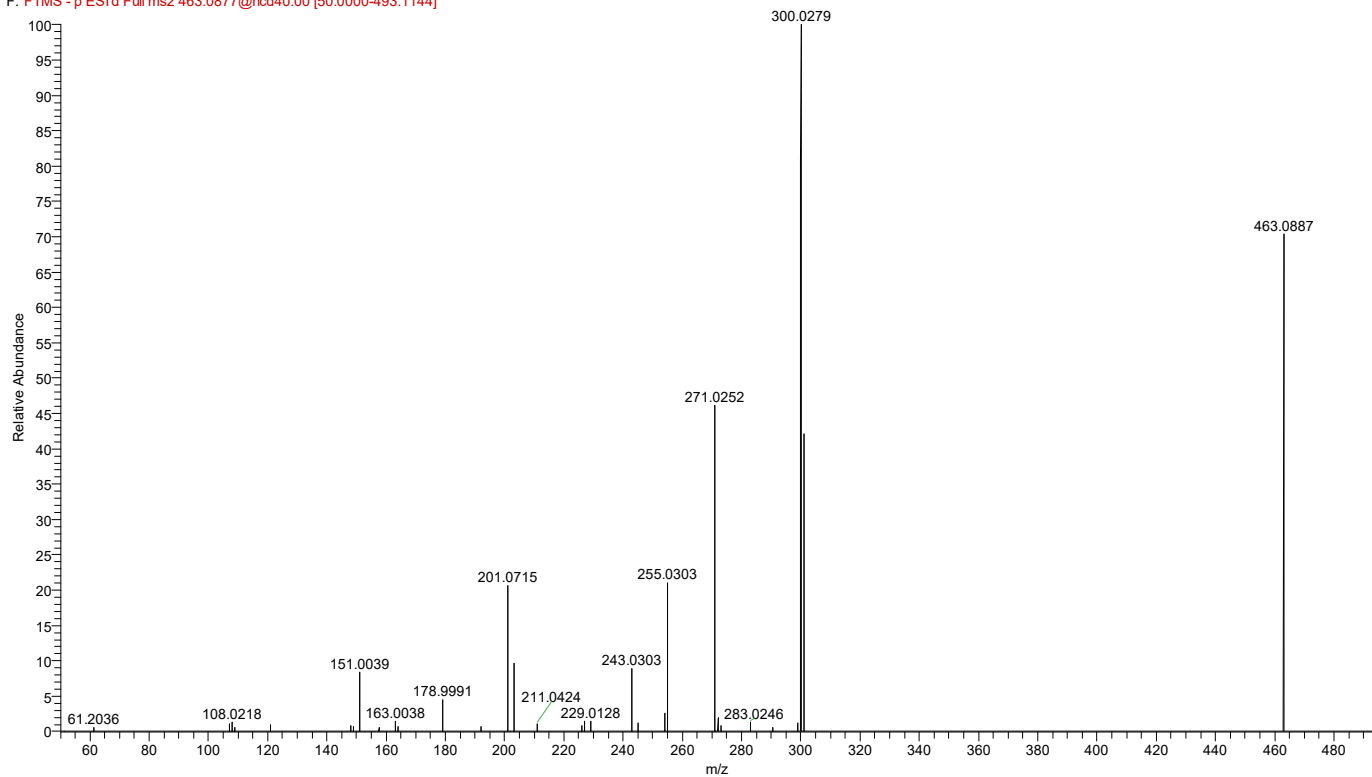


Figure S9. MS² fragmentation spectra (CID) of quercetin-3 β -D-glucoside

ANX-100%JC-Pd #12781 RT: 11.14 AV: 1 NL: 6.41E5
F: FTMS + p ESI:d Full ms2 303.0498@hcd40.00 [50.0000-329.8758]

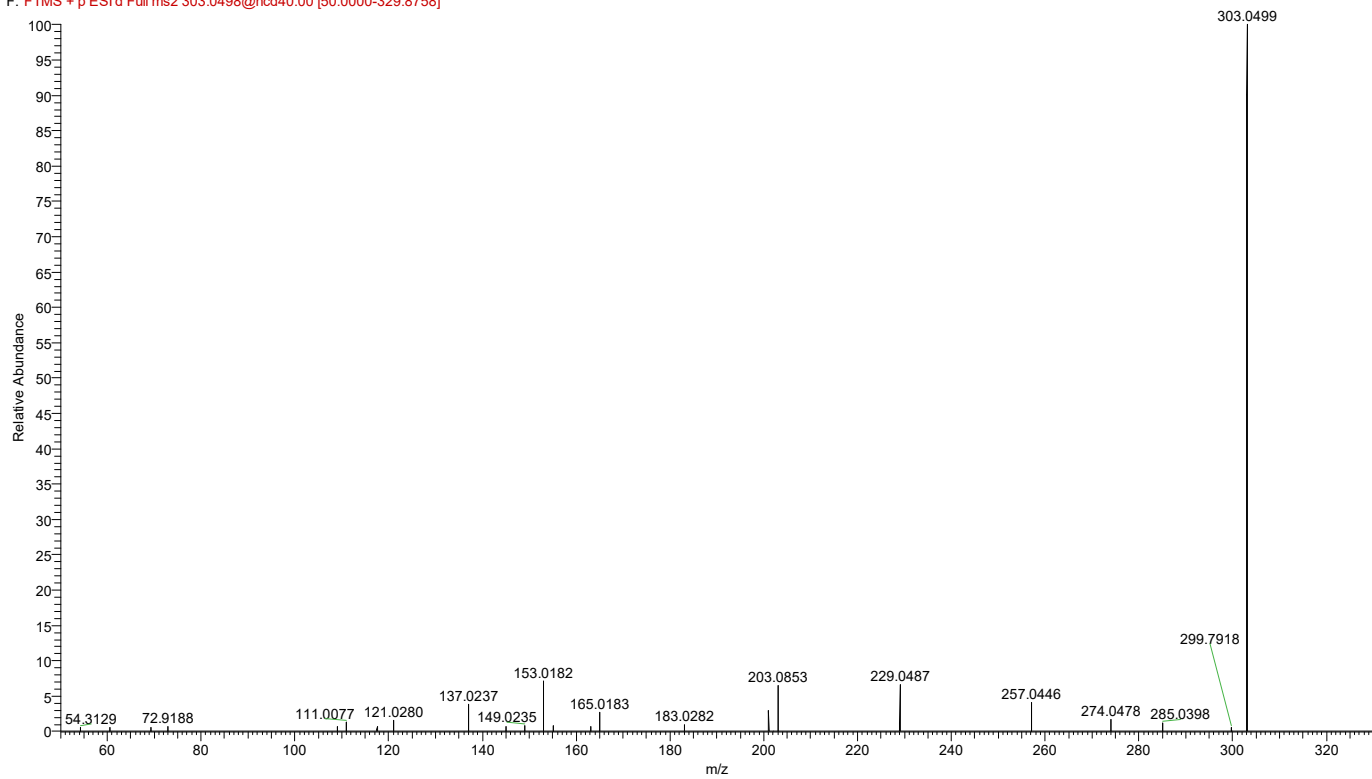


Figure S10. MS² fragmentation spectra (CID) of quercetin

ANX-100%JC-Nd #13649 RT: 12.05 AV: 1 NL: 2.77E5
F: FTMS - p ESId Full ms2 433.0110@hcd40.00 [50.0000-462.4362]

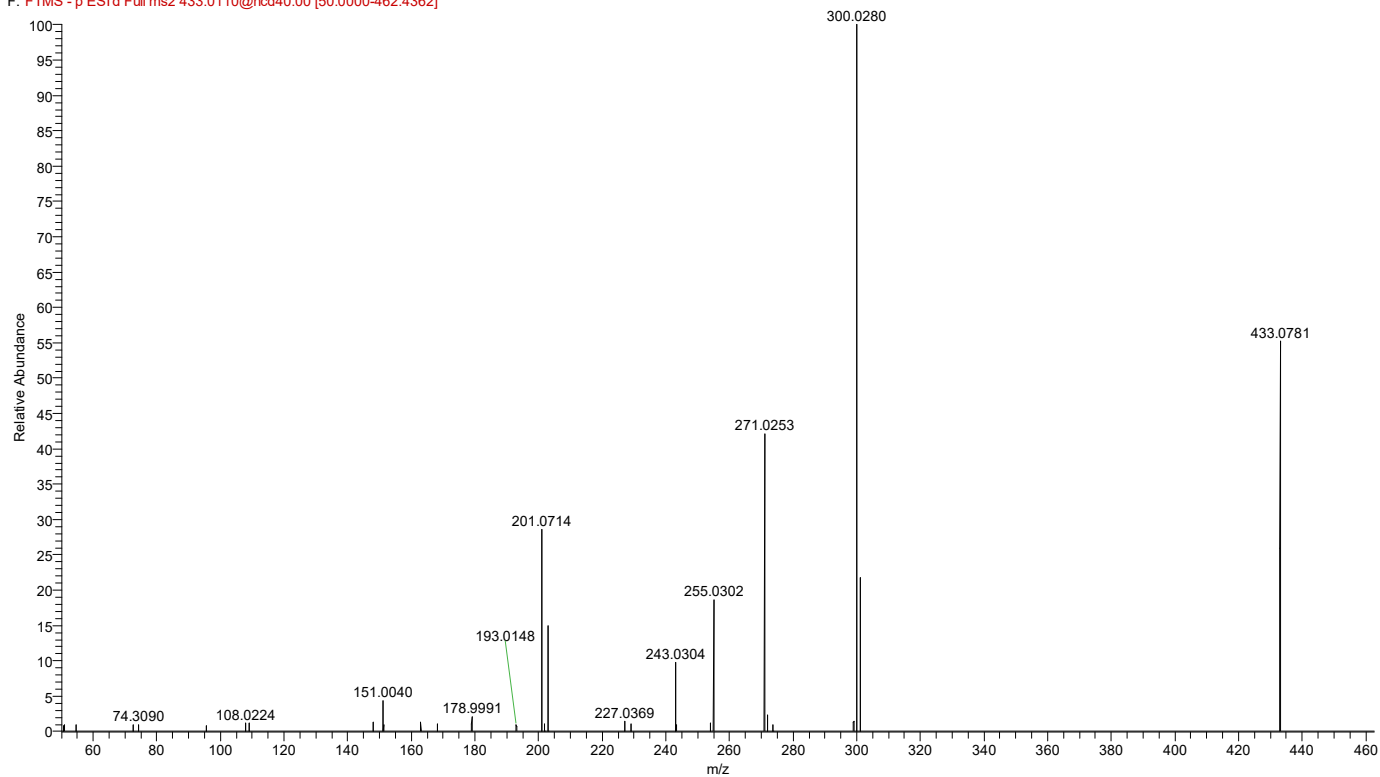


Figure S11. MS² fragmentation spectra (CID) of quercetin-3-Arabinoside

ANX-100%JC-Nd #13684 RT: 12.08 AV: 1 NL: 4.08E5
F: FTMS - p ESId Full ms2 447.0297@hcd40.00 [50.0000-476.7353]

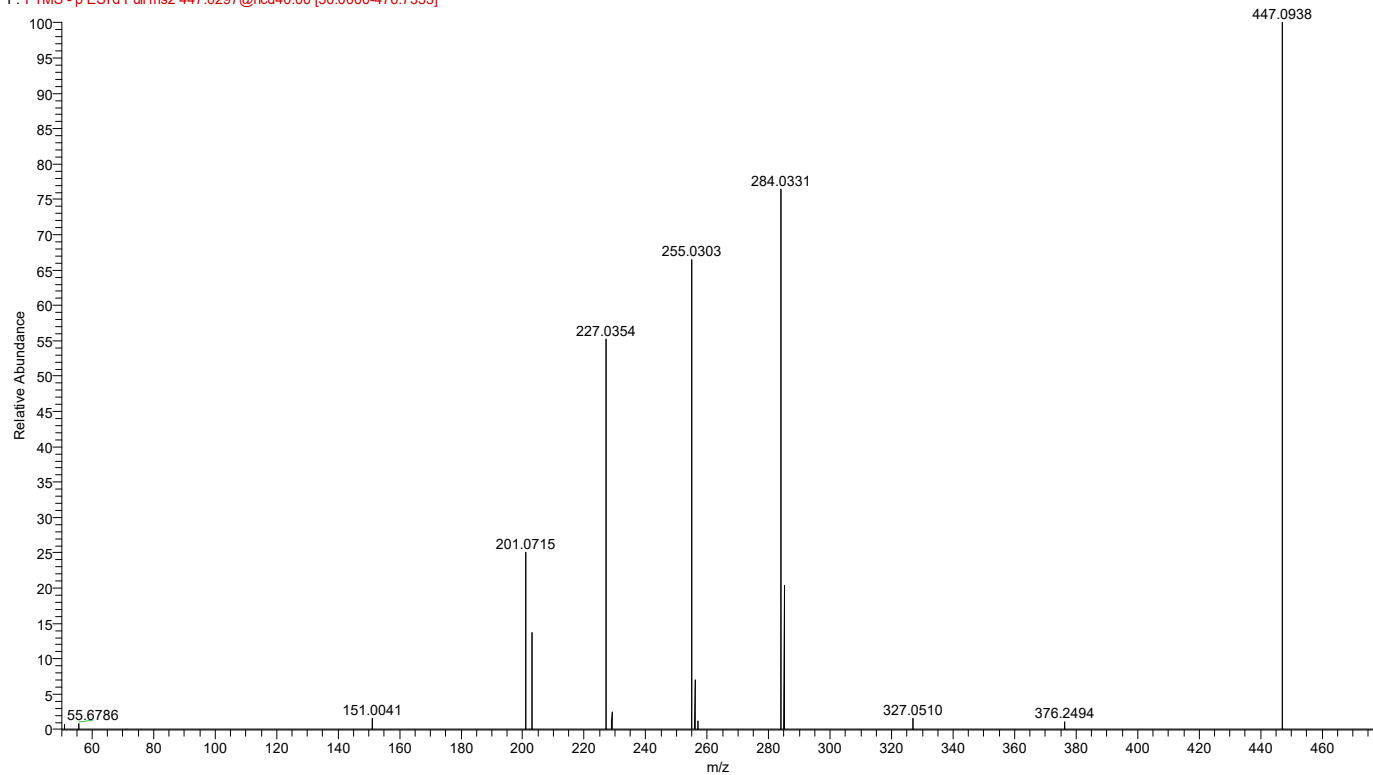


Figure S12. MS² fragmentation spectra (CID) of cynaroside

ANX-100%JC-Nd #14166 RT: 12.50 AV: 1 NL: 1.39E5
F: FTMS - p ESId Full ms2 515.1196@hcd40.00 [54.6187-546.1871]

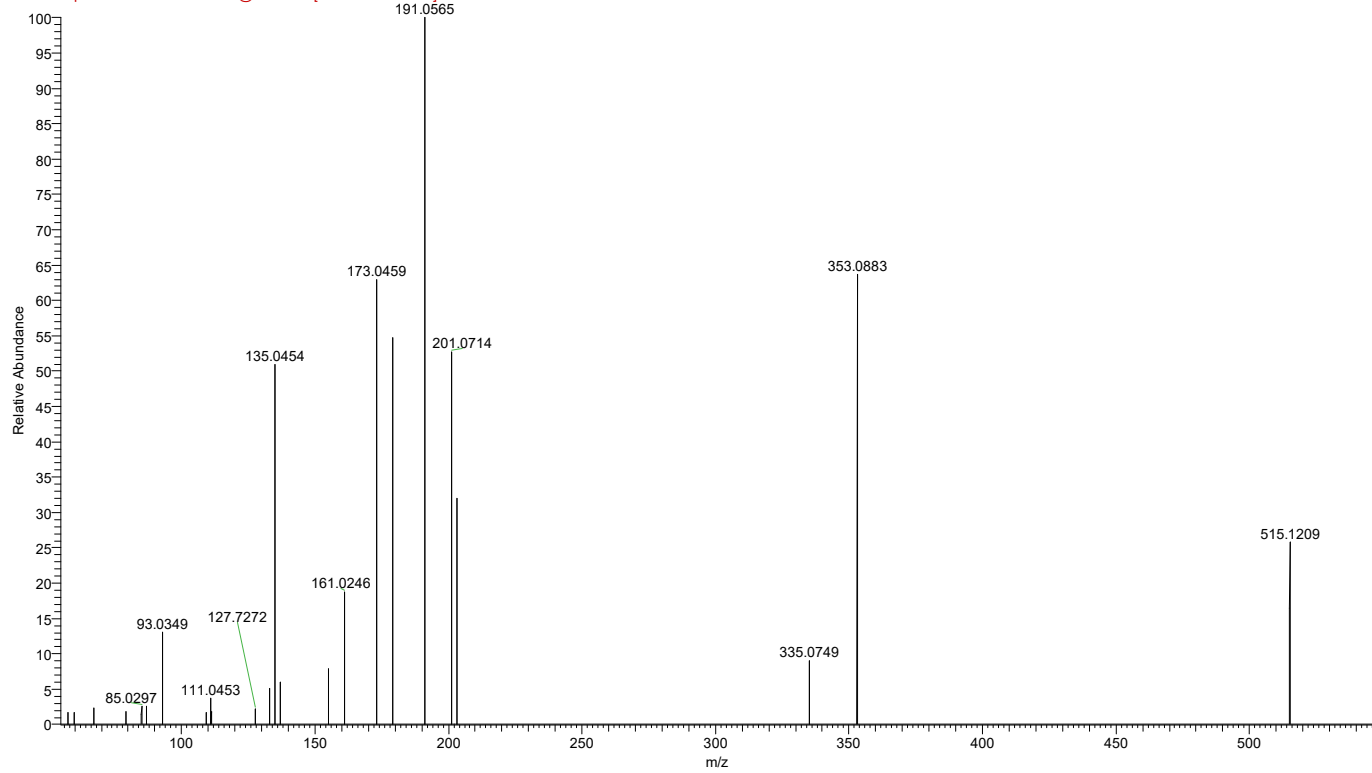


Figure S13. MS² fragmentation spectra (CID) of 1,3–Dicaffeoylquinic acid

ANX-100%JC-Nd #14371 RT: 12.68 AV: 1 NL: 6.78E5
F: FTMS - p ESId Full ms2 353.0871@hcd40.00 [50.0000-380.9139]

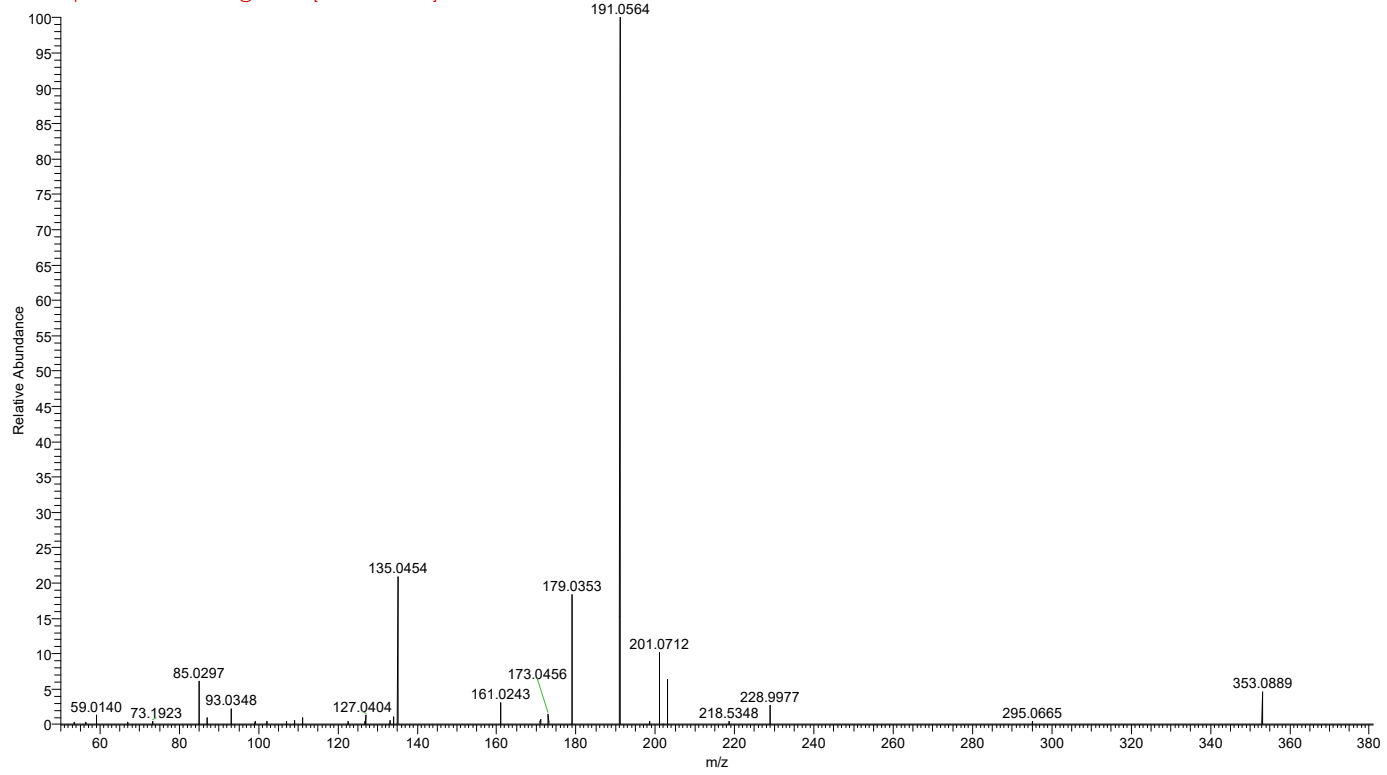


Figure S14. MS² fragmentation spectra (CID) of chlorogenic acid

ANX-100%JC-Nd #14806 RT: 13.07 AV: 1 NL: 1.01E5
F: FTMS - p ESI:d Full ms2 477.1795@hcd40.00 [50.7488-507.4881]

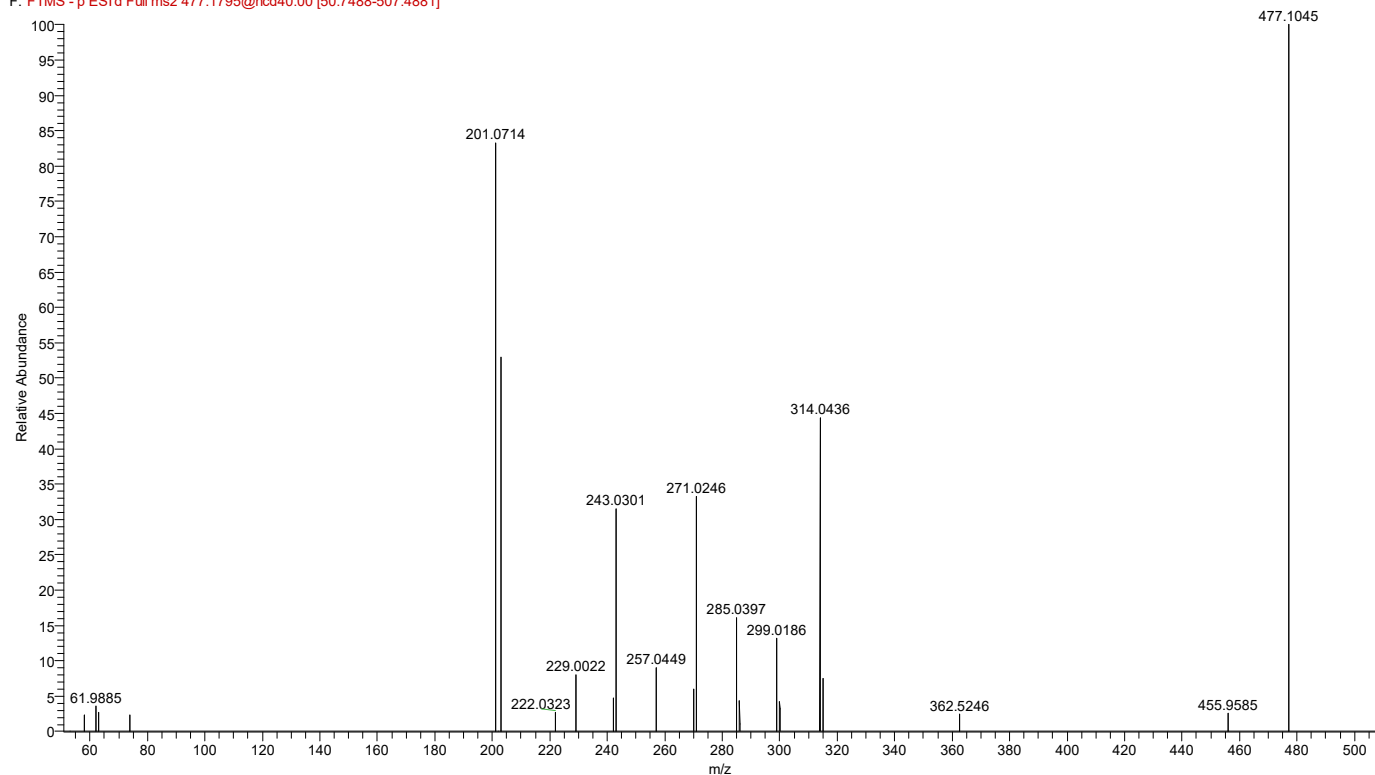


Figure S15. MS² fragmentation spectra (CID) of isorhamnetin-3-O-glucoside

ANX-100%JC-Pd #15453 RT: 13.47 AV: 1 NL: 1.29E6
F: FTMS + p ESI:d Full ms2 193.0498@hcd40.00 [43.5352-217.6758]

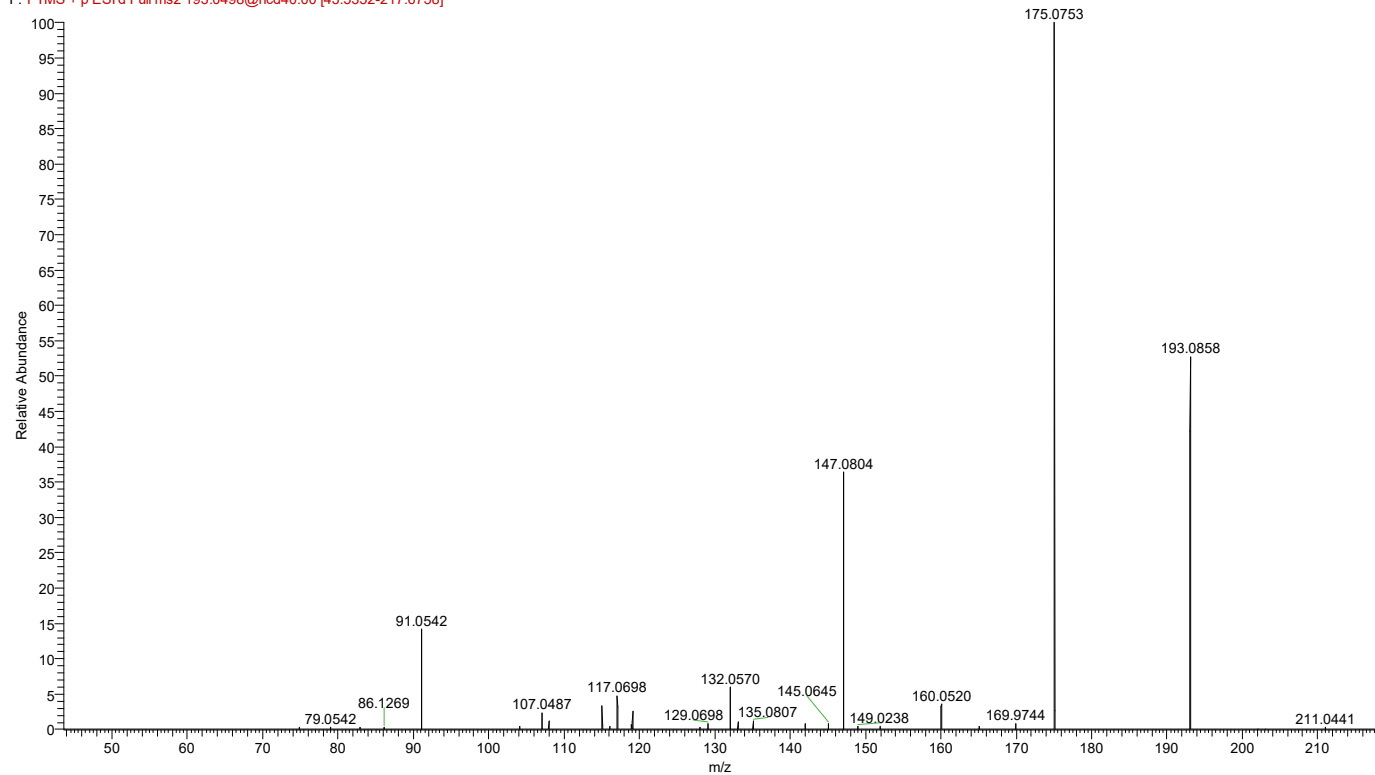


Figure S16. MS² fragmentation spectra (CID) of 4-oxo-5-phenylpentanoic acid

ANX-100%JC-Nd #18449 RT: 16.28 AV: 1 NL: 4.94E6
F: FTMS - p ESId Full ms2 287.0438@hcd40.00 [50.0000-313.5497]

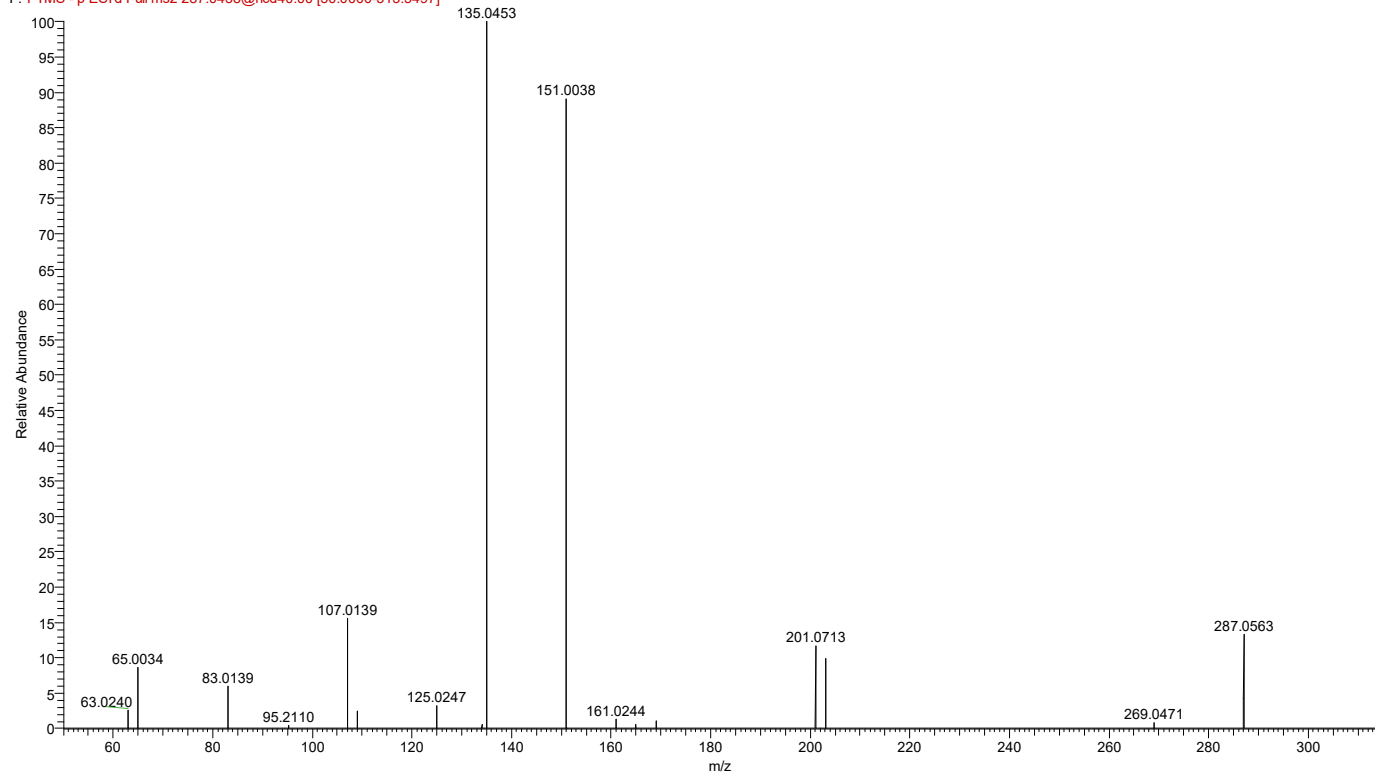


Figure S17. MS² fragmentation spectra (CID) of eriodictyol

ANX-100%JC-Nd #20150 RT: 17.78 AV: 1 NL: 1.20E5
F: FTMS - p ESId Full ms2 317.0050@hcd40.00 [50.0000-344.1101]

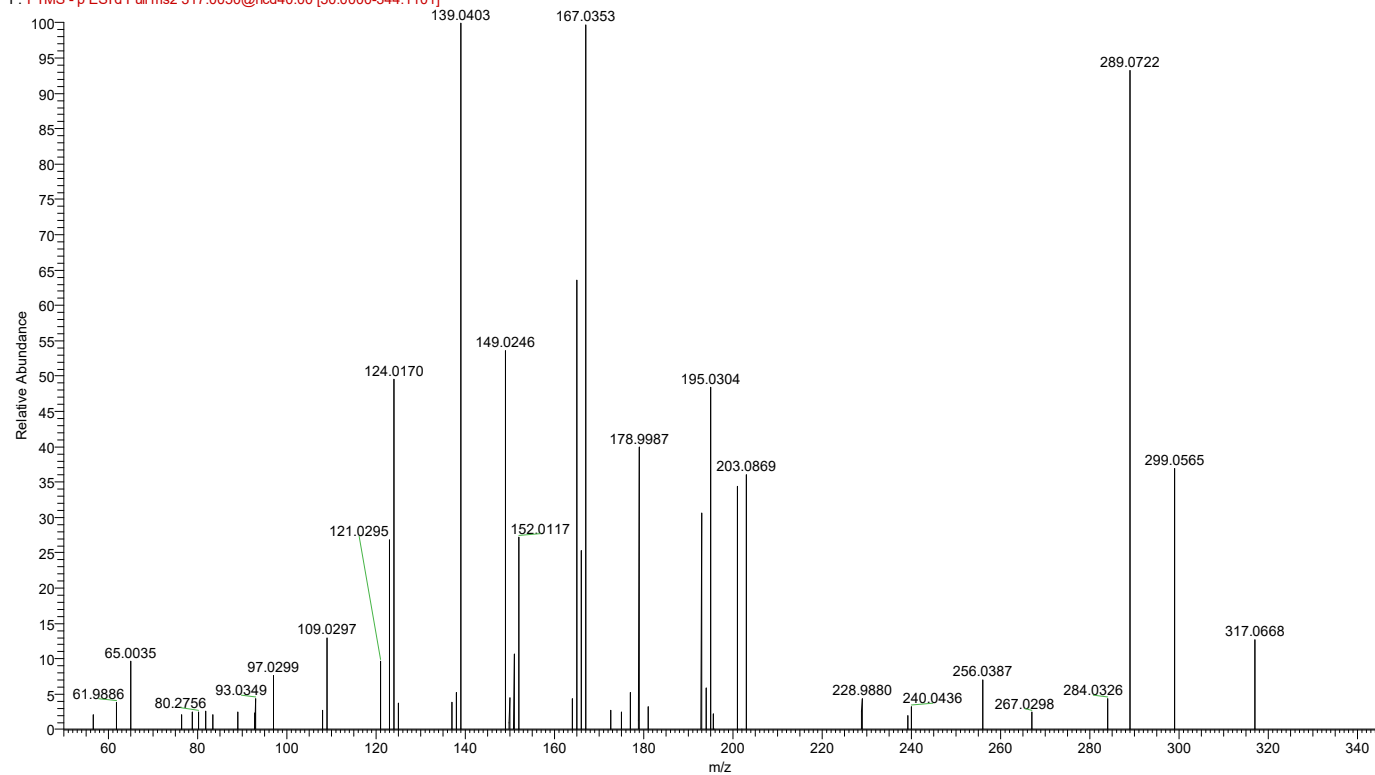


Figure S18. MS² fragmentation spectra (CID) of padmatin

ANX-100%JC-Nd #20340 RT: 17.95 AV: 1 NL: 8.66E5
F: FTMS - p ESId Full ms2 315.0504@hcd40.00 [50.0000-342.1164]

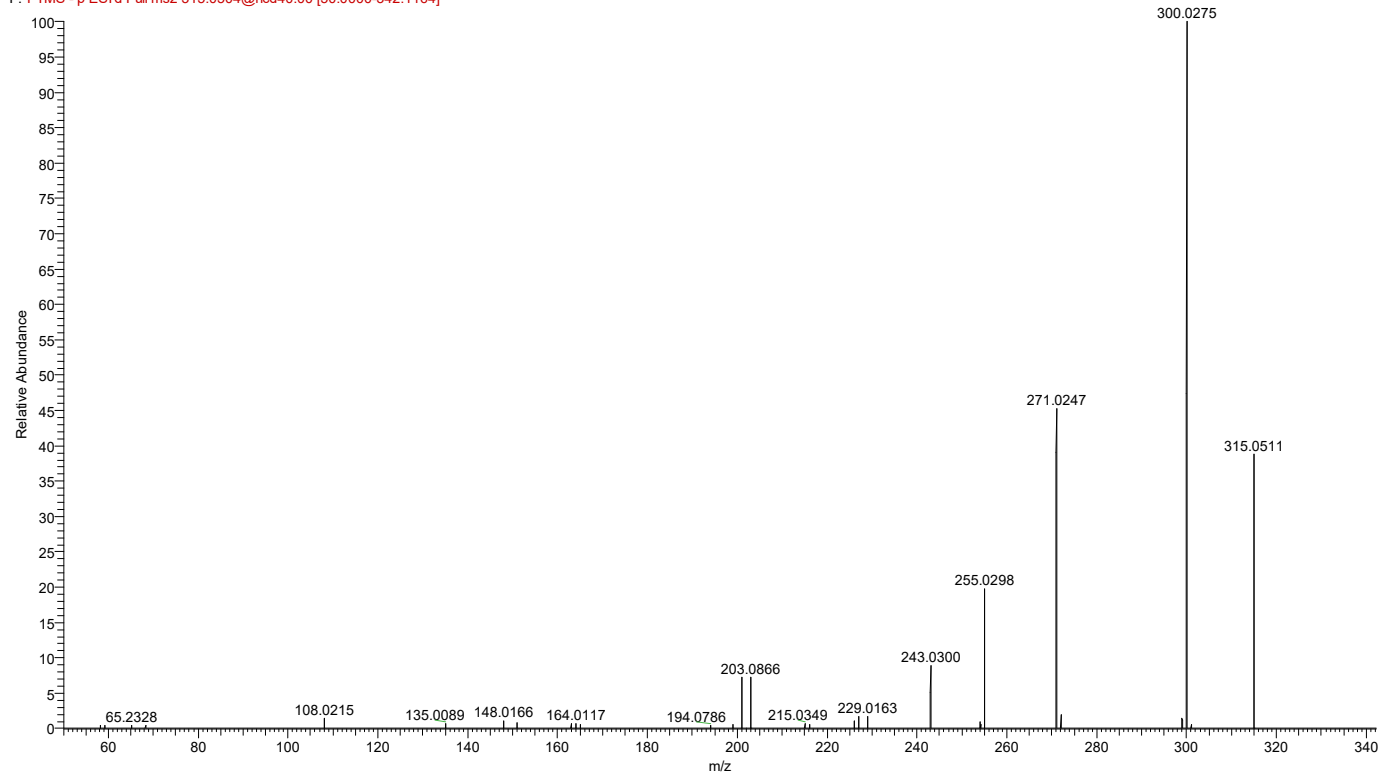


Figure S19. MS² fragmentation spectra (CID) of isorhamnetin

ANX-100%JC-Nd #20830 RT: 18.39 AV: 1 NL: 4.52E5
F: FTMS - p ESId Full ms2 271.0612@hcd40.00 [50.0000-297.2475]

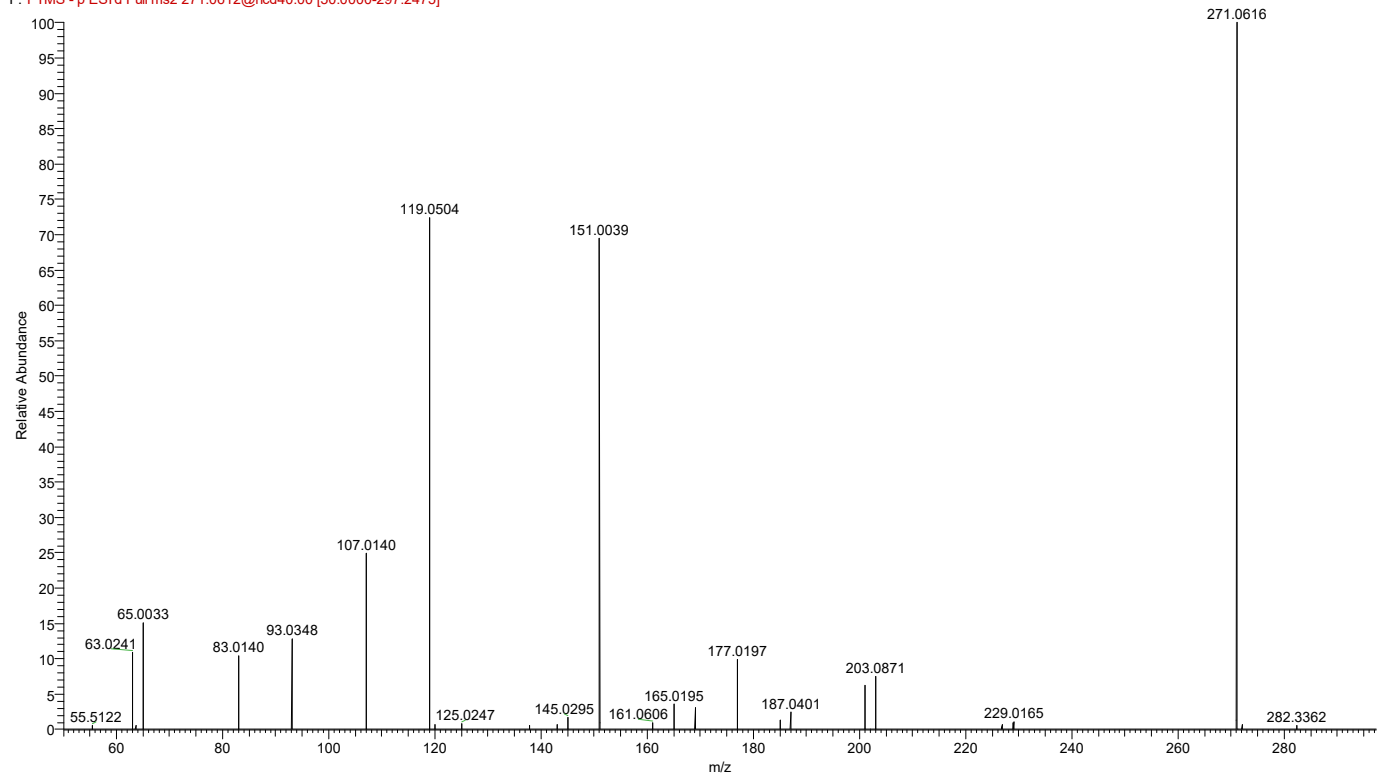


Figure S20. MS² fragmentation spectra (CID) of naringenin

ANX-100%JC-Pd #21939 RT: 19.12 AV: 1 NL: 1.19E5
F: FTMS + p ESI Full ms2 303.0498@hcd40.00 [50.0000-329.8758]

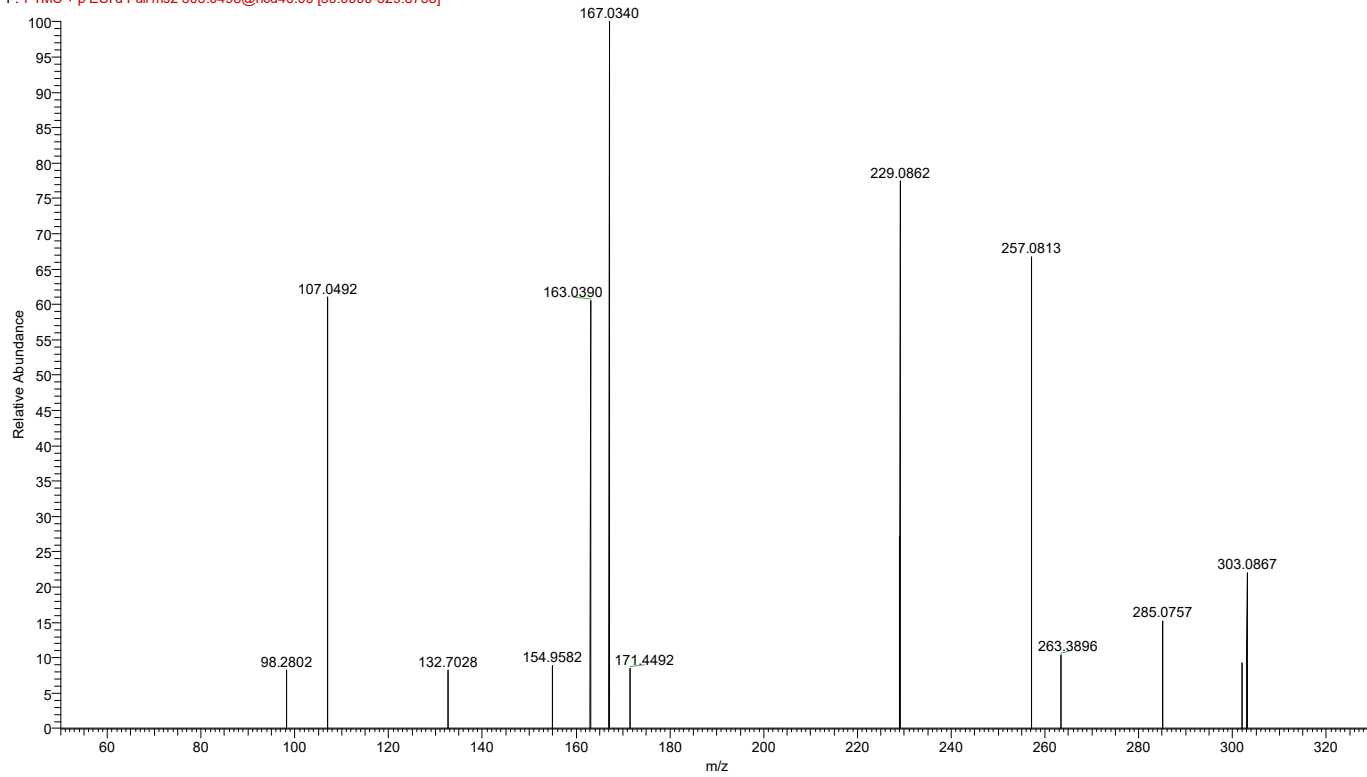


Figure S21. MS² fragmentation spectra (CID) of 7-O-Methylaromadendrin

ANX-100%JC-Pd #22293 RT: 19.43 AV: 1 NL: 2.59E6
F: FTMS + p ESI Full ms2 331.0812@hcd40.00 [50.0000-358.4678]

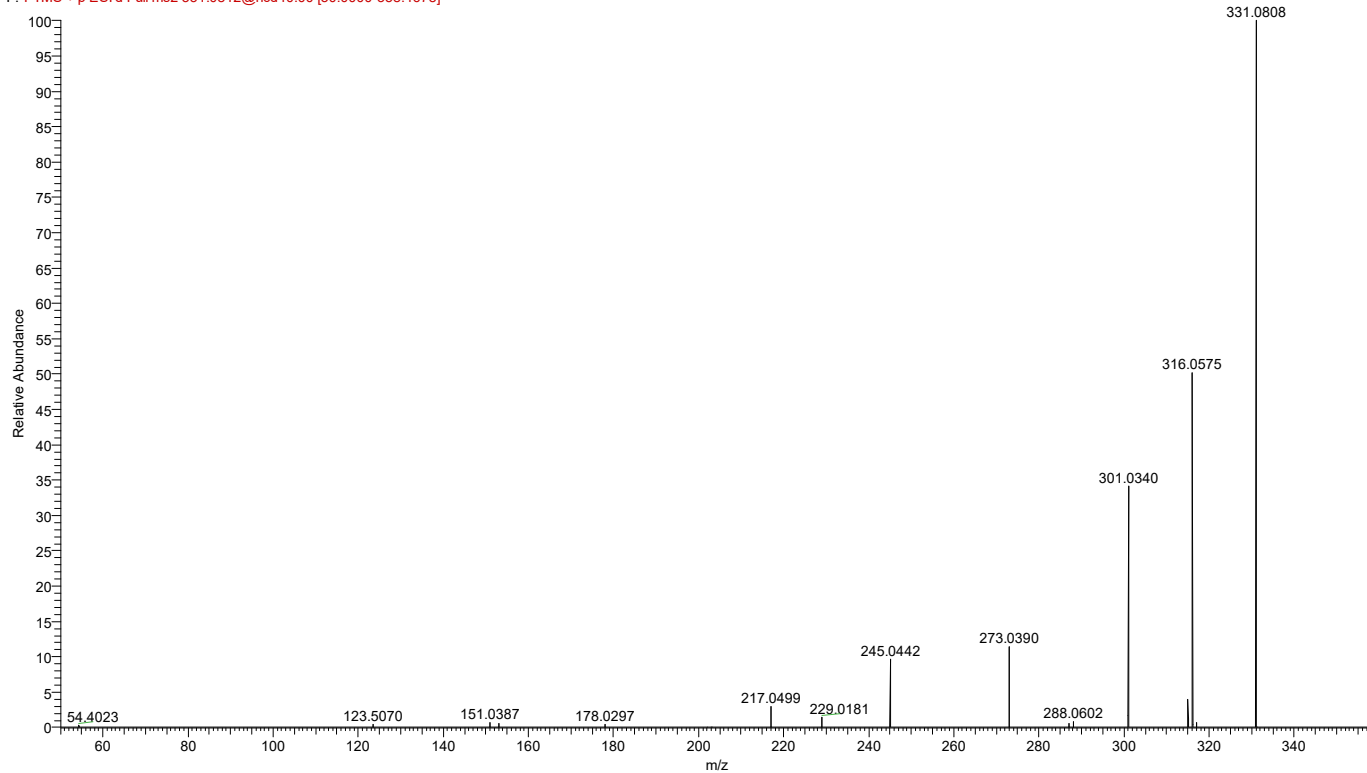


Figure S22. MS² fragmentation spectra (CID) of aurantio-obtusin

ANX-100%JC-Pd #22218 RT: 19.36 AV: 1 NL: 6.01E5
F: FTMS + p ESId Full ms2 209.0809@hcd40.00 [46.8055-234.0275]

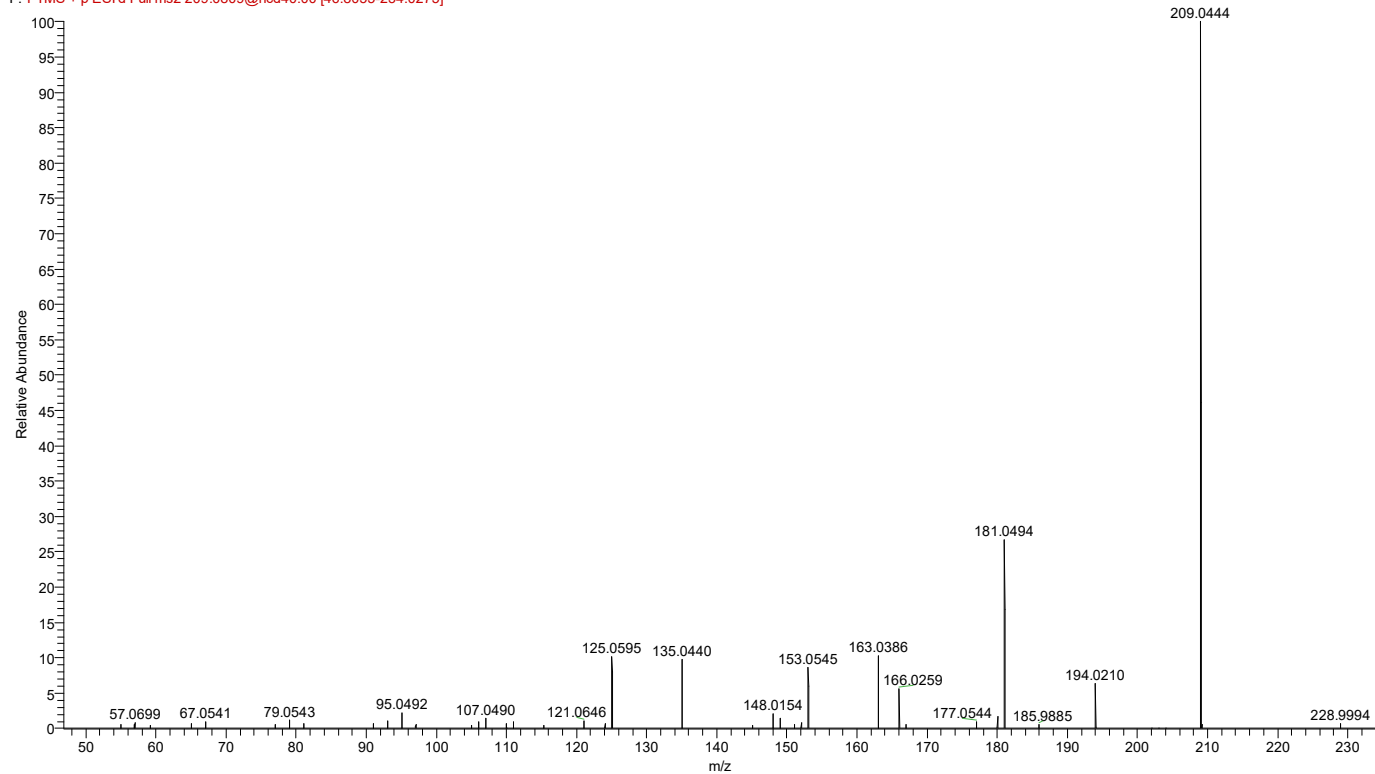


Figure S23. MS² fragmentation spectra (CID) of fraxetin

ANX-100%JC-Nd #22430 RT: 19.80 AV: 1 NL: 2.52E7
F: FTMS - p ESId Full ms2 301.0712@hcd40.00 [50.0000-327.8576]

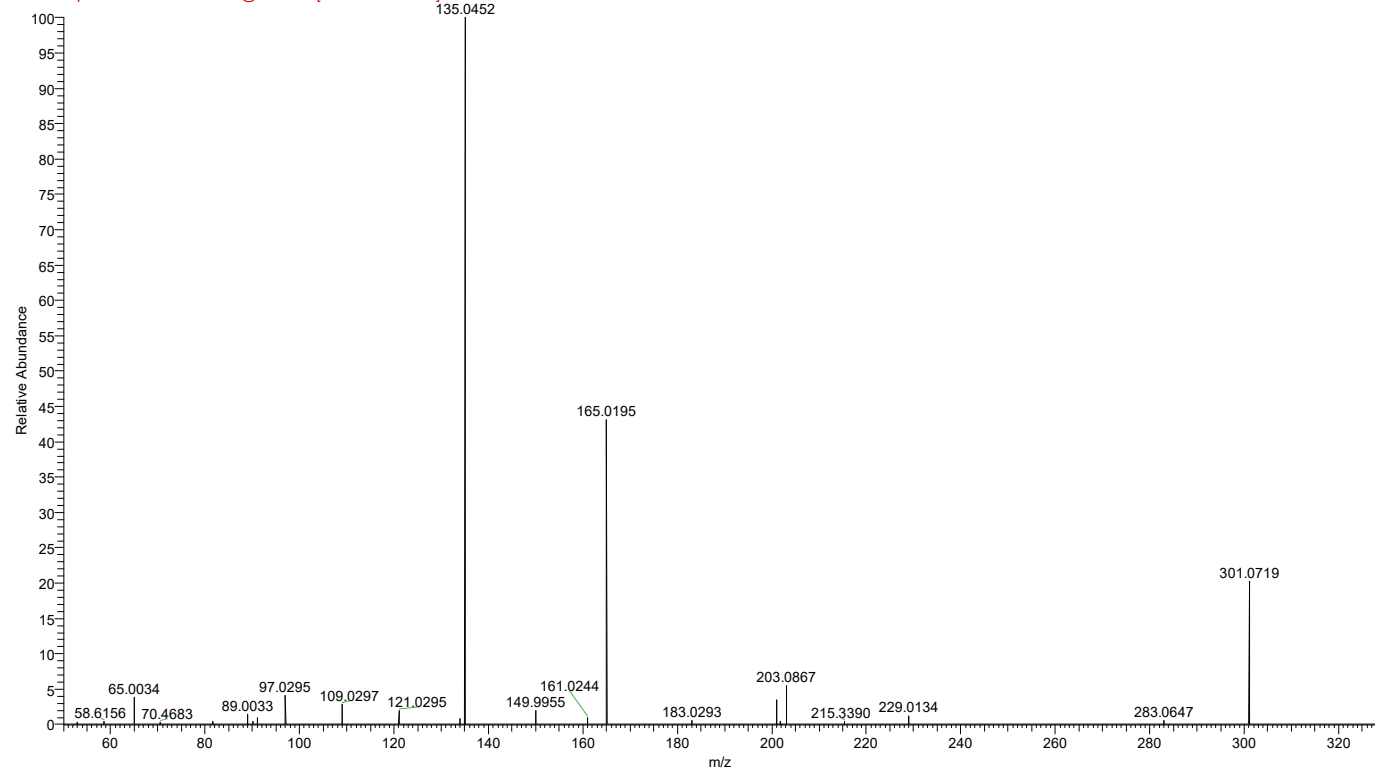


Figure S24. MS² fragmentation spectra (CID) of hematoxylin

ANX-100%JC-Pd #23704 RT: 20.66 AV: 1 NL: 1.72E6
F: FTMS + p ESI d Full ms2 287.0552@hcd40.00 [50.0000-313.5613]

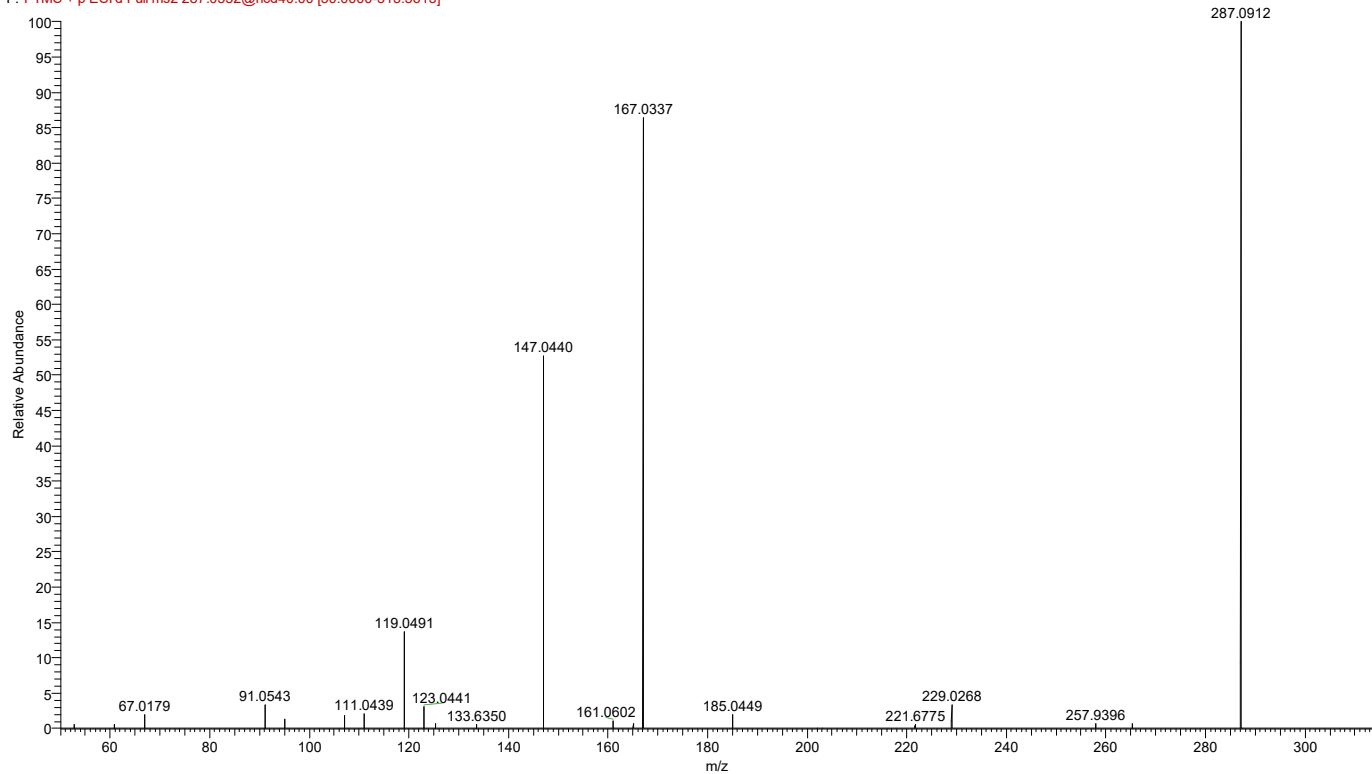


Figure S25. MS² fragmentation spectra (CID) of sakuranetin

ANX-100%JC-Pd #24688 RT: 21.51 AV: 1 NL: 8.11E6
F: FTMS + p ESI d Full ms2 445.2120@hcd40.00 [50.0000-474.8813]

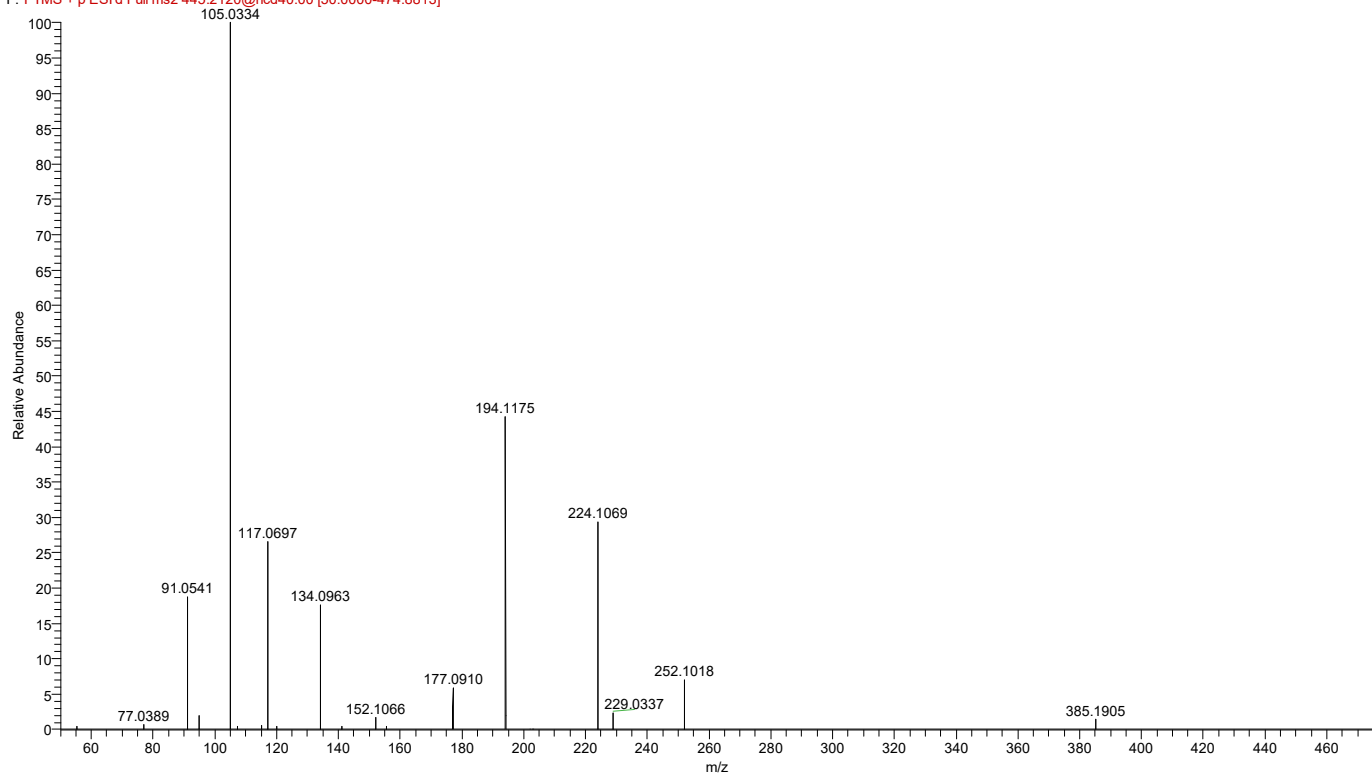


Figure S26. MS² fragmentation spectra (CID) of aurantiamide acetate

ANX-100%JC-Pd #26440 RT: 23.04 AV: 1 NL: 1.83E5
F: FTMS + p ESI d Full ms2 297.1484@hcd40.00 [50.0000-323.8564]

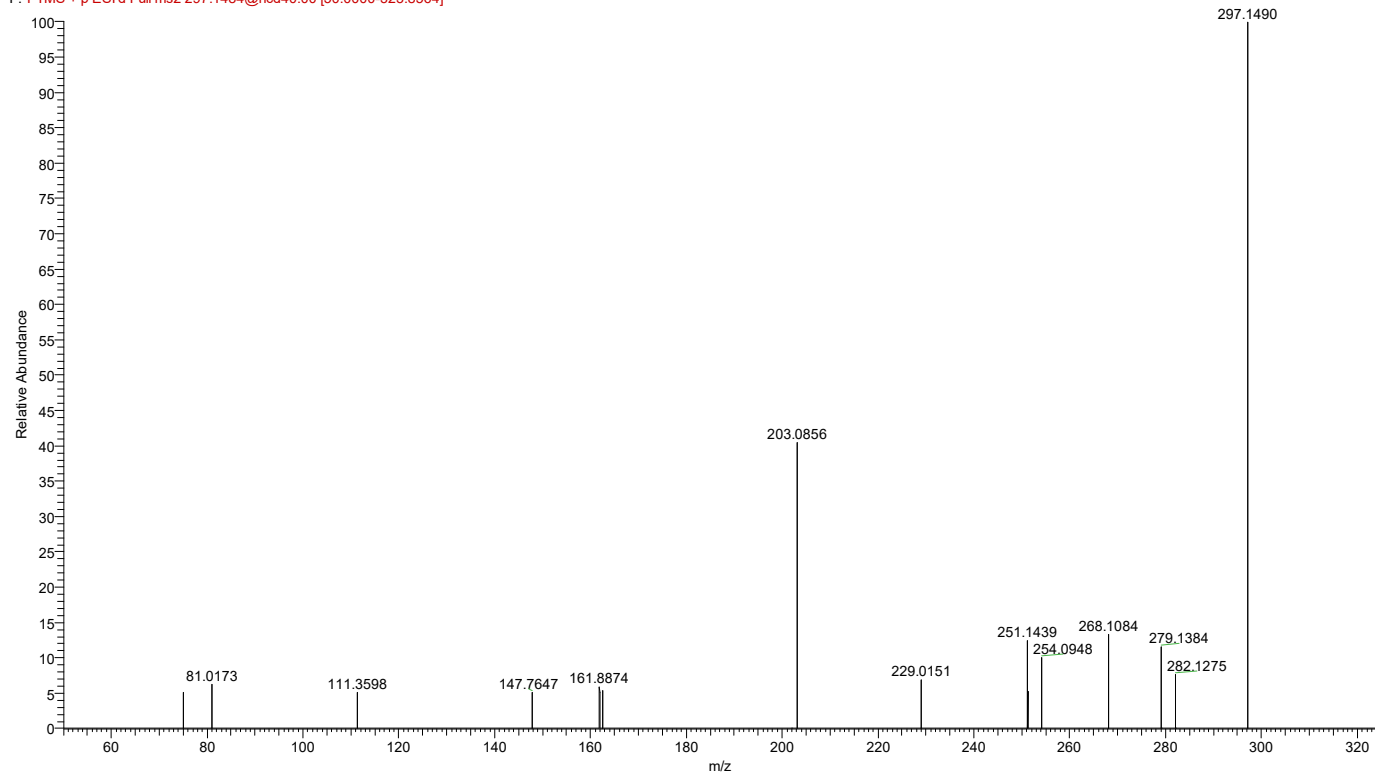


Figure S27. MS² fragmentation spectra (CID) of cryptotanshinone

ANX-100%JC-Pd #26678 RT: 23.24 AV: 1 NL: 1.05E6
F: FTMS + p ESI d Full ms2 219.1743@hcd40.00 [48.8646-244.3228]

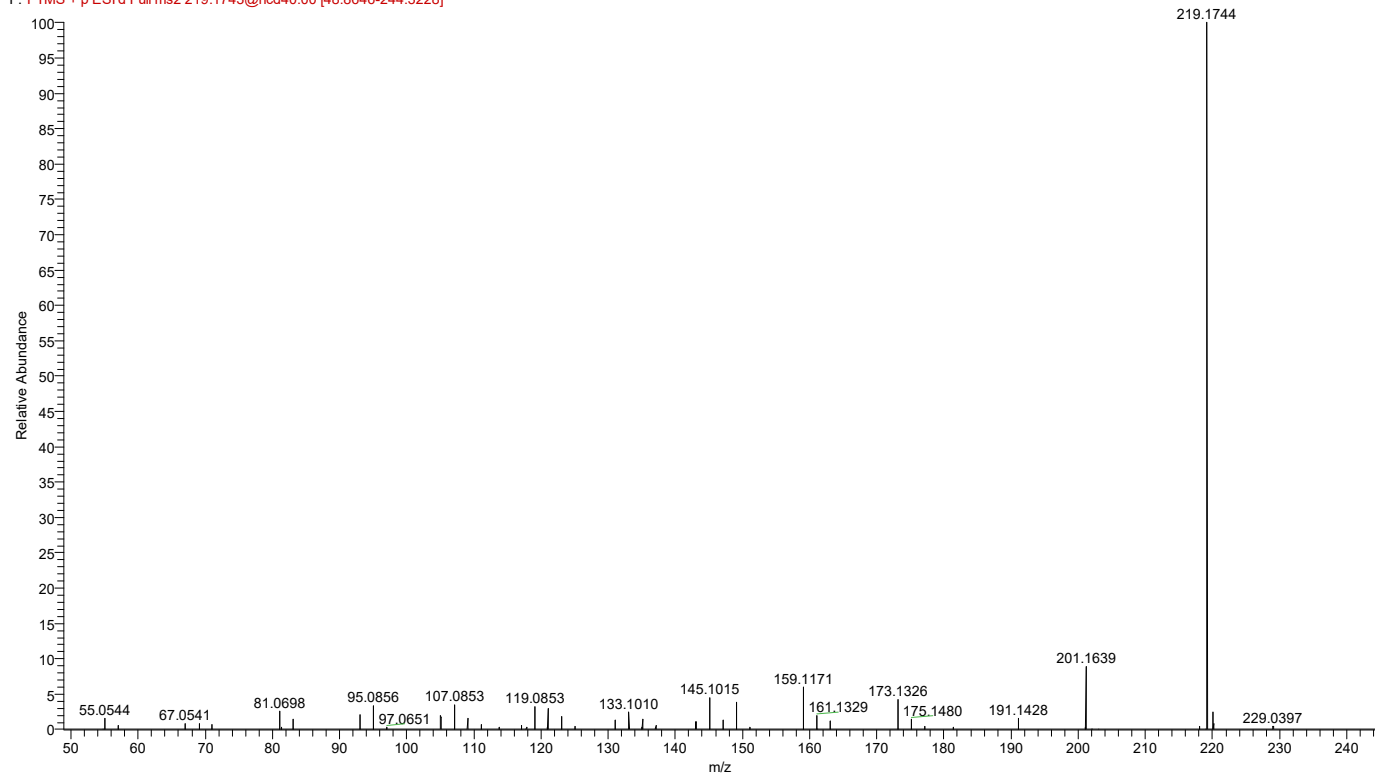


Figure S28. MS² fragmentation spectra (CID) of nootkatone

ANX-100%JC-Pd #26723 RT: 23.28 AV: 1 NL: 1.85E6
F: FTMS + p ESI d Full ms2 220.1694@hcd40.00 [49.0676-245.3378]

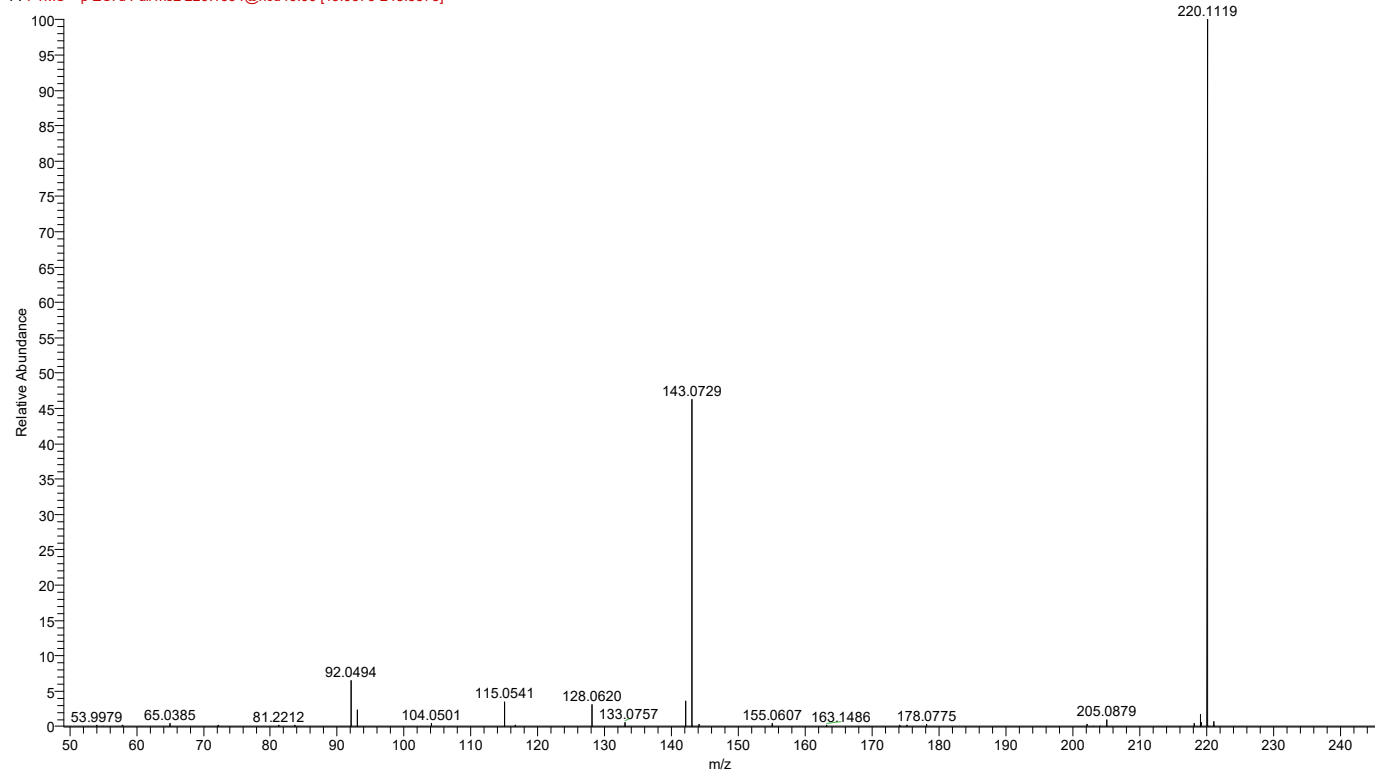


Figure S29. MS² fragmentation spectra (CID) of N-Phenyl-1-naphthylamine

ANX-100%JC-Pd #27625 RT: 24.07 AV: 1 NL: 2.00E5
F: FTMS + p ESI d Full ms2 295.1904@hcd40.00 [50.0000-321.8592]

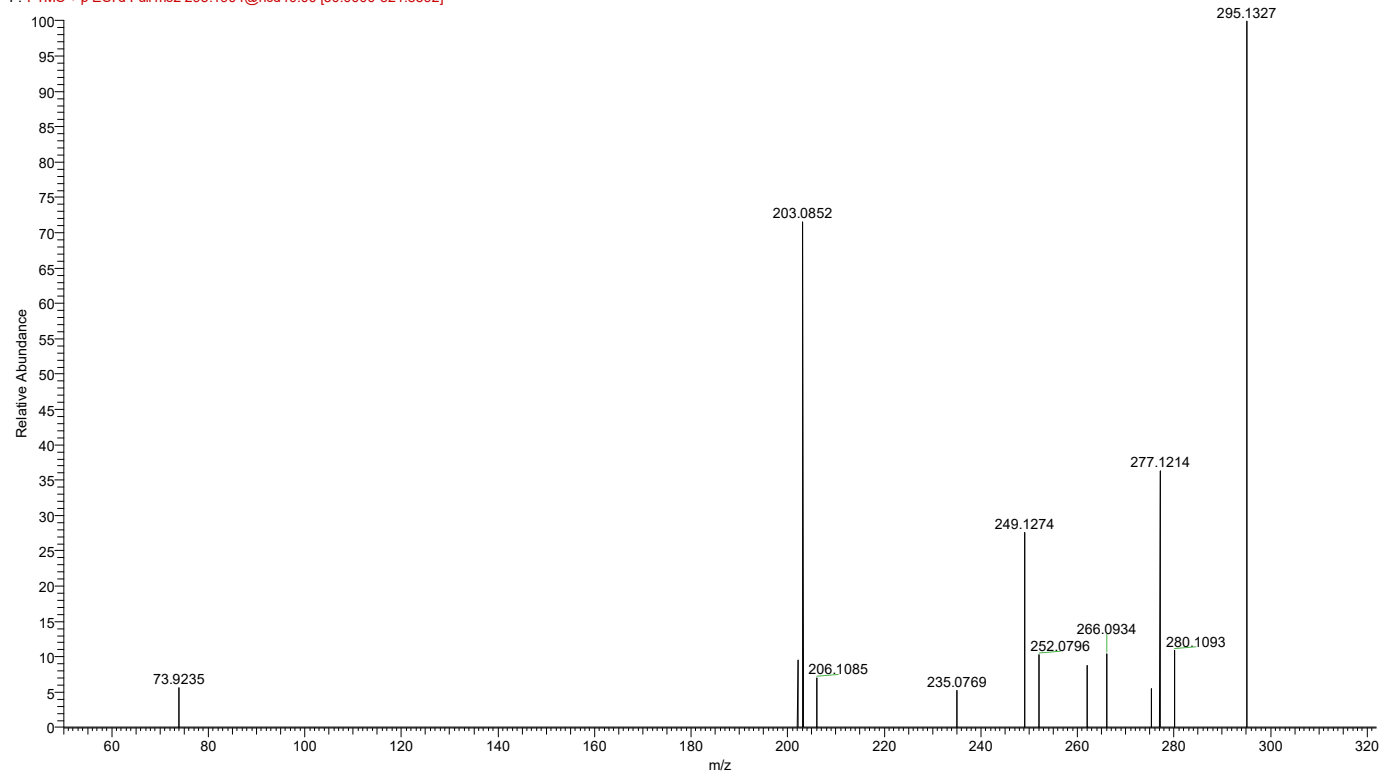


Figure S30. MS² fragmentation spectra (CID) of tanshinone IIA

ANX-100%JC-Pd #28354 RT: 24.70 AV: 1 NL: 6.52E5
F: FTMS + p ESI Full ms2 403.2398@hcd40.00 [50.0000-432.0696]

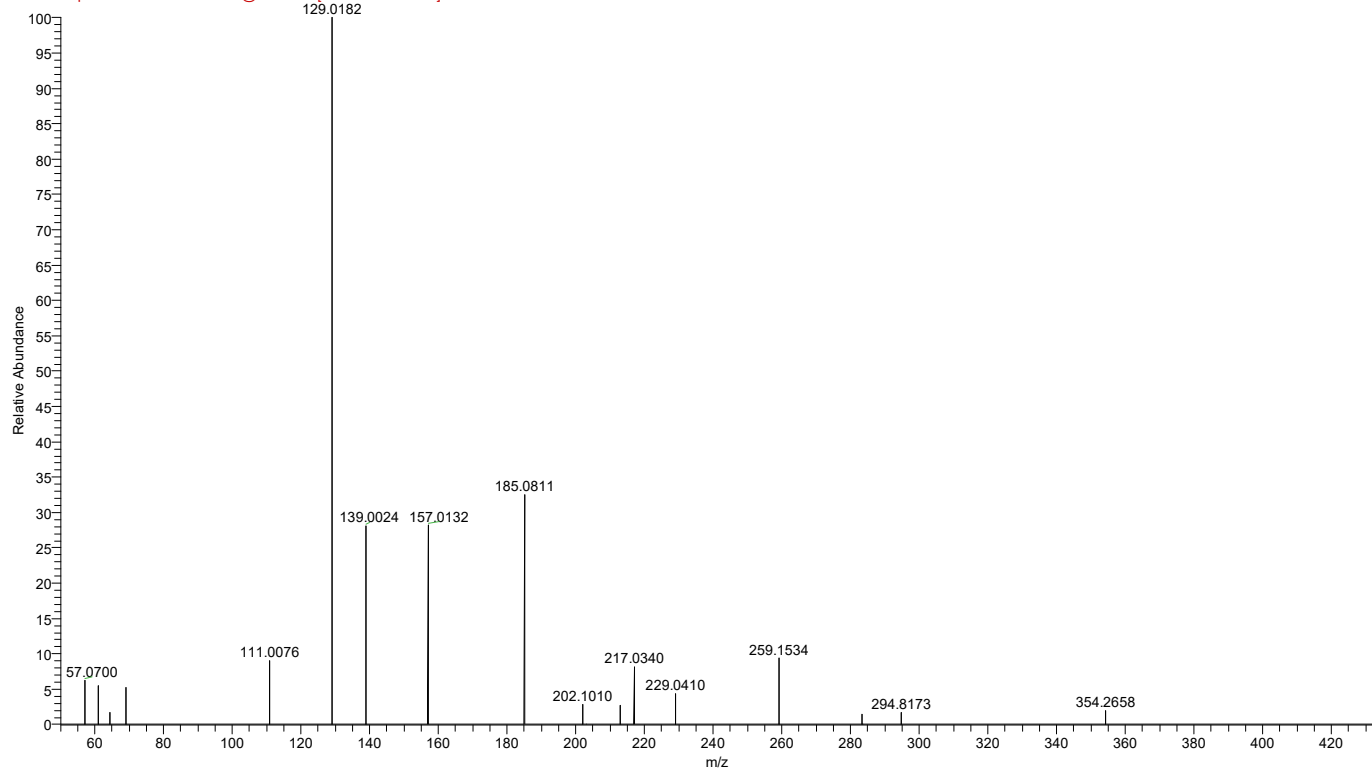


Figure S31. MS² fragmentation spectra (CID) of citroflex A-4

RT: 0.00 - 29.01 SM: 5G

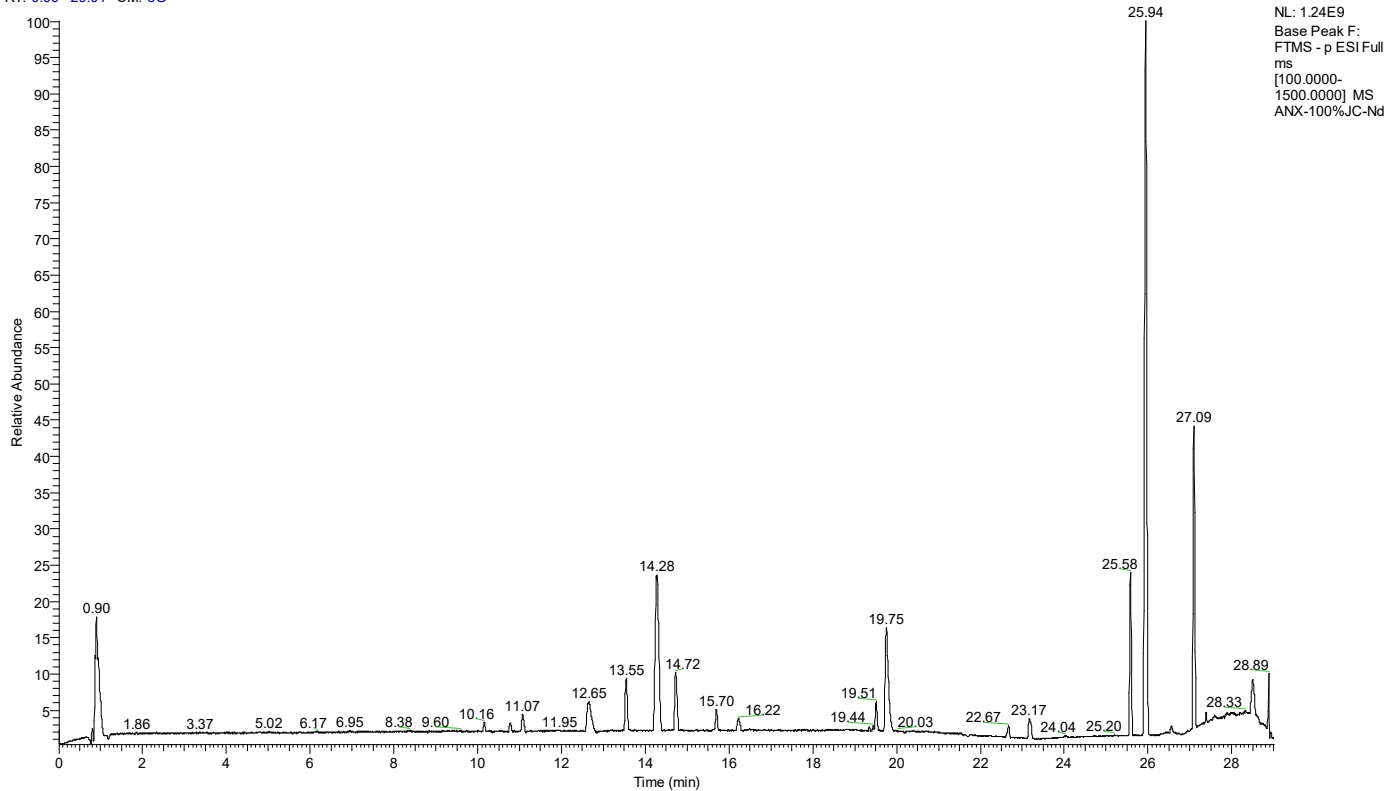


Figure S32. TICs of *Blumea balsamifera* (L.) DC. in negative ion mode

RT: 0.00 - 29.01 SM: 5G

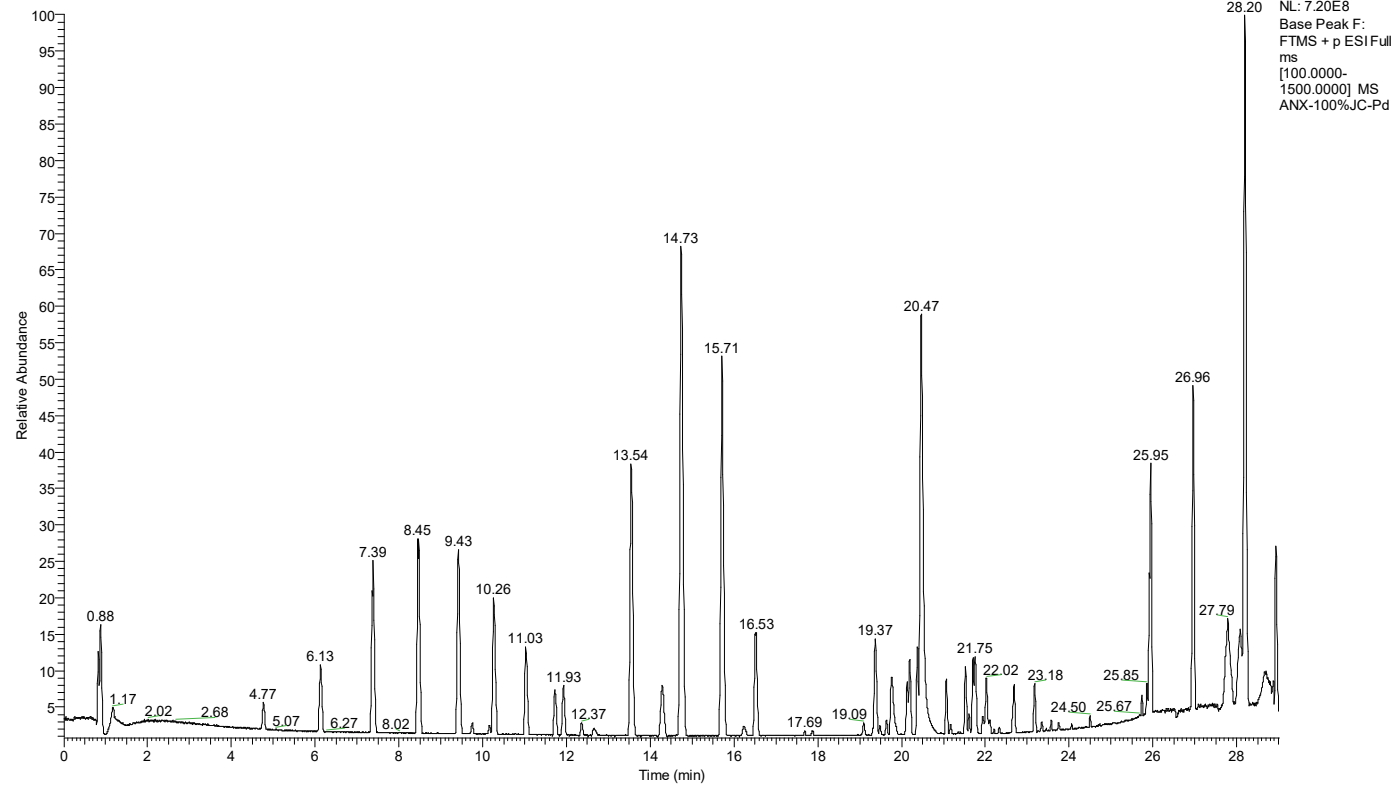


Figure S33. TICs of *Blumea balsamifera* (L.) DC. in positive ion mode